INFORMATION TO USERS

This manuscript has been reproduced from the microfilm master. UMI films the text directly from the original or copy submitted. Thus, some thesis and dissertation copies are in typewriter face, while others may be from any type of computer printer.

The quality of this reproduction is dependent upon the quality of the copy submitted. Broken or indistinct print, colored or poor quality illustrations and photographs, print bleedthrough, substandard margins, and improper alignment can adversely affect reproduction.

In the unlikely event that the author did not send UMI a complete manuscript and there are missing pages, these will be noted. Also, if unauthorized copyright material had to be removed, a note will indicate the deletion.

Oversize materials (e.g., maps, drawings, charts) are reproduced by sectioning the original, beginning at the upper left-hand corner and continuing from left to right in equal sections with small overlaps.

Photographs included in the original manuscript have been reproduced xerographically in this copy. Higher quality 6" x 9" black and white photographic prints are available for any photographs or illustrations appearing in this copy for an additional charge. Contact UMI directly to order.

ProQuest Information and Learning
300 North Zeeb Road, Ann Arbor, MI 48106-1346 USA
800-521-0600

University of Alberta

Direct measurement of accumulation and localization of cadmium in giant algal cells of *Chara corallina*

by

Matthew Joseph Bryman 

A thesis submitted to the Faculty of Graduate Studies and Research in partial fulfillment of the requirements for the degree of Master of Science

in

Plant Biology
Department of Biological Sciences

Edmonton, Alberta
Spring 2002

University of Alberta

Library release form

Name of Author: Matthew Joseph Bryman

Title of Thesis: Direct measurement of accumulation and localization of cadmium in giant algal cells of *Chara corallina*

Degree: Master of Science

Year this Degree Granted: Spring 2002

Matthew Bryman

4454 w 7th Avenue
Vancouver BC, V6R 1W9

Date: Jan 30, 2002

University of Alberta

Faculty of Graduate Studies and Research

The undersigned certify that they have read, and recommended to the Faculty of Graduate Studies and Research for acceptance, a thesis entitled **Direct measurement of accumulation and localization of cadmium in giant algal cells of *Chara corallina*** submitted by **Matthew Joseph Bryman** in partial fulfillment of the requirements for the degree of **Master of Science** in **Plant Biology**.

Dr. Gregory J. Taylor

Dr. Jeffrey Goldberg

Dr. Larry Fliegel

Date thesis approved by committee: Jan 24, 2002

Abstract

Cadmium (Cd) has gained worldwide attention due to bioaccumulation in crop plants. One step towards limiting Cd bioaccumulation is through a thorough understanding of subcellular Cd localization. Previous studies with root tissue have utilized indirect analytical approaches to assign pools of Cd to specific subcellular locations. I have directly measured Cd accumulation and localization using *Chara corallina* as a model system, where individual cells can be isolated and surgically separated into distinct subcellular components (cell wall, protoplasm, and vacuole). Following exposure, the majority of Cd accumulated in the cell wall, and accumulation occurred by both metabolism-dependent and independent processes. Cadmium accumulation in the total protoplasm was metabolism-dependent, and was approximately equal in the avacuolate protoplasm and the vacuole. Desorption profiles suggested multiple Cd binding sites were present in the cell wall. Results reported here challenge assumptions regarding Cd accumulation and localization from previous studies. A re-examination may be warranted.

Acknowledgements

There are many people I would like to thank for their help during preparation of this thesis and throughout my graduate degree. First, I would like to thank Dr. Gregory Taylor for the opportunity to work in his research group, and his continual support and guidance during my stay in the lab. The members of my supervisor committee, Dr. Jeffrey Goldberg and Dr. Larry Fliegel, are thanked for their helpful comments and suggestions. I am extremely grateful to all members of the Taylor lab for making my graduate experience a memorable one, and I am indebted to both Julie McDonald-Stephens and Dr. Neil Harris for their time, patience, and invaluable assistance. Finally, I would like to acknowledge the funding and support of the Department of Biological Sciences in the form of a Teaching Assistantship, and the funding received by Dr. Gregory Taylor by the Natural Sciences and Engineering Research Council of Canada.

Table of Contents

List of Tables

List of Figures

Chapter 1: A review of research examining cadmium accumulation and localization.

1.1. Cadmium contamination, human health, and economic concerns

Cadmium (Cd) is receiving increasing worldwide attention due to its presence as a contaminant on agricultural lands, and bioaccumulation in consumable organs of crop plants such as rice (Homma and Hirata 1984), wheat, sunflower, flax, and potatoes (Grant *et al.* 1997). Introduction of Cd into the environment occurs from a variety of industrial processes including steel and alloy production, use of pigments and stabilizers in plastics, Ni-Cd battery production, and Zn smelting (Little and Martin 1972, Eklund 1995, Alloway 1997). However, inputs of Cd to agricultural soils are mostly due to applications of municipal sewage sludge as a fertilizer (Ryan *et al.* 1982, Chaney *et al.* 1996), contamination in phosphatic fertilizer applications (Roberts 1996), and aerial contamination from industrial emissions (Alloway 1997). Once in the soil, Cd has a long residence time (15 – 1100 yrs, Alloway 1997), supporting the observation of increasing soil Cd levels over time (Jones *et al.* 1992). Understanding the relationship between Cd in the environment and bioaccumulation in plants is of critical importance as human exposure occurs primarily through smoking and food intake. Regardless of the source, chronic exposure to Cd can lead to detrimental effects on human health (Jarvis *et al.* 1976, Nordberg 1996).

Concerns for human health problems arising from Cd accumulated by plants from agricultural lands were first raised upon identification of Cd as an etiological factor in Itai-itai disease (Nordberg 1996). Itai-itai disease (affecting residents of Japan after the Second World War) is characterized by long term exposure to Cd in conjunction with low intake of essential nutrients and low vitamin D synthesis, resulting in kidney and bone disease. Chronic accumulation of Cd in kidneys, irrespective of diet, has also been found to result in renal dysfunction if levels exceed 200 mg kg^{-1} tissue (Ryan *et al.* 1982, Alloway 1997). Human dietary intake of Cd is estimated to range from 25-75 $\mu g\ day^{-1}$. This is close to the World Health Organization recommended limit of 70 $\mu g\ day^{-1}$ (Choudhary *et al.* 1995). In an effort to reduce Cd exposure in the human diet,

international limits of 0.1 mg Cd kg^{-1} are under consideration as a maximum tolerable level for exported cereals, pulses and legumes (Codex Alimentairus Commissions 2000). Formal adoption of this limit may have an impact on the export of Canadian wheat as the median Cd concentration of durum wheat grain samples in Alberta was above the proposed limit from 1991–1999 (Canadian grain commission, unpublished results). Unless changes in crop culture or agronomic practices occur, economic losses could be substantial (estimated $1.1 billion 1994–1995).

The level of Cd transferred from soil to crops, and then from crops to humans is still a highly debated topic. Crops grown on soils low in Cd have resulted in a high incidence of Cd-induced disease in Japan and China, while no disease has been reported in persons ingesting crops grown elsewhere in soils 25–250 times richer in Cd (Chaney *et al.* 1996). Environmental conditions in rice growing regions (low zinc (Zn) and iron (Fe) levels in soils) have been implicated in higher plant Cd accumulation, while reduced levels of Zn and Fe in the diet have been implicated in higher transfer rates to humans (Chaney *et al.* 1996). These conditions do not extend to the remainder of the worlds' population and croplands, raising questions about actual levels of Cd transferred from crops to humans. Regardless of this debate, crops grown on slightly contaminated soils can accumulate Cd levels exceeding proposed limits, increasing the potential for transfer to humans (Grant *et al.* 1997). A thorough understanding of Cd accumulation processes in plants is a necessary step towards limiting Cd bioaccumulation by crops, and reducing the potential for accumulation by humans following consumption.

1.2. Accumulation of cadmium by plants

The majority of plant Cd exposure occurs in the soil, at the soil/root interface. Once Cd is accumulated in the root it can be mobilized to above ground, consumable organs. This provides a port of entry into the human diet. Numerous processes can influence the amount of Cd found in grains or seeds. At the soil/root interface, the availability of Cd is affected by factors including total Cd in the soil, the equilibrium between Cd in the soil solid phase versus soil solution, soil pH, and speciation of Cd (Alloway 1997). The physical mechanisms of Cd movement from soil to root symplasm are not fully

understood, although it has been suggested that metal transport proteins facilitate movement across the plasma membrane (Reid *et al.* 1999). In support of this argument, numerous metal transport proteins in plants with the ability to transport Cd have been characterized. Genes encoding transport proteins include wheat *LCT1* (Clemens *et al.* 1998), and the *Arabidopsis thaliana CAX2* (Hirschi *et al.* 2000) and *AtNramp* gene family (Thomine *et al.* 2000). Evidence exists to suggest expression of a high-affinity Cd transporter in *Thlaspi caerulescens*, but it has yet to be cloned (Lombi *et al.* 2001). Also a Cd^{2+}/H^{+} exchanger at the tonoplast of oat root vesicles has been suggested (Salt and Wagner 1993), but not cloned. These proteins appear to have varying affinities for different metal ions, and could serve as multi-cation transporters. For example, the transporter encoded by *LCT1* also transports Ca^{2+} (Clemens *et al.* 1998), *AtNramp* family gene products also transport Fe (Thomine *et al.* 2000), and the *CAX2* product appears to transport Ca^{2+} and Mn^{2+} (Hirschi *et al.* 2000). This evidence supports the hypothesis that Cd gains entry to the symplasm or vacuole by acting as an analogue to nutrient cations (Jarvis *et al.* 1976).

Once plant entry has been achieved, Cd is thought to move from the root system to the shoot in the xylem and subsequently to the grains or seeds in the phloem. Movement of Cd in the xylem/phloem may be affected by similar factors (pH, Cd concentration and speciation) that affect Cd movement from soil to roots. In addition, movement in the xylem/phloem may reflect differential Cd levels available for mobilization, possibly due to sequestration of Cd in tissues, organs or organelles. For example, Cd has been detected in tonoplast vesicles from oats (Salt and Wagner 1993), but the potential for sequestration was not explored. The *CAX2* gene product is also associated with the tonoplast. This supports a metal ion sequestration hypothesis, as expression of *CAX2* in tobacco increased Mn^{2+} tolerance (Hirschi *et al.* 2000). Other investigations of mobilization to the shoot have demonstrated both inter-specific (Jarvis *et al.* 1976) and intra-specific (Boggess *et al.* 1978, Florjin *et al.* 1993) variation.

Apart from transfer to consumable organs, Cd has been shown to have detrimental effects on numerous plant physiological processes. These include inhibition of

photosystem I and II reactions in tomato (Baszynski *et al.* 1980) and wheat (Atal *et al.* 1991), decreased membrane permeability in rice leading to alterations in plant nutritional status (Llamas *et al.* 1998), and reduced CO_2 fixation and carbon metabolism in wheat seedlings (Malik *et al.* 1992). These effects can lead to decreased plant productivity, and may eventually decrease yield if Cd concentrations are sufficiently high.

1.3. Quantification of subcellular cadmium levels

In an effort to understand movement of Cd into plants, numerous studies have attempted to quantify total and intracellular Cd levels and the kinetics of Cd accumulation in plant roots. Total accumulation is concentration-dependent in roots of wheat (Hart *et al.* 1998), rice (Homma and Hirata 1984), soybean (Cataldo *et al.* 1983), white lupin (Costa and Morel 1993), and the green algae *Chlorella pyrenoidosa* (Hart *et al.* 1979). Accumulation is inhibited by the presence of divalent cations, including Mn^{2+} (Hart *et al.* 1979, Cataldo *et al.* 1983, Garnham *et al.* 1992), Cu^{2+}, Fe^{2+} (Cataldo *et al.* 1983), Zn^{2+} (Cataldo *et al.* 1983, Garnham *et al.* 1992, Costa and Morel 1993), and Mg^{2+} (Garnham *et al.* 1992). This result is not surprising due to similarities in the chemical and ionic characteristics of these cations (Table 1.1). Competitive inhibition is in agreement with Cd acting as an analogue of nutrient cations to gain entry into the symplasm (Jarvis *et al.* 1976). Lower K_m values for Cd compared with Zn^{2+}, Fe^{2+}, and Cu^{2+} (Cataldo *et al.* 1983, Homma and Hirata 1984) further support this hypothesis, as does the identification and cloning of various multi-cation transport proteins (Clemens *et al.* 1998, Hirschi *et al.* 2000, Thomine *et al.* 2000).

While research investigating Cd accumulation has improved our understanding of total uptake and accumulation rates, reliable partitioning of accumulated Cd into external (apoplasm) and internal (symplasm) components has not been achieved. This reflects a reliance on indirect analytical approaches, collecting data from whole root experiments (organ level) and interpreting results at the cellular level. Two indirect approaches have been employed to quantify Cd found in the apoplasm and symplasm. One approach, exemplified by the work of Cataldo *et al.* (1983) and Hart *et al.* (1998), involved the

examination of Cd accumulation in roots when exposed to Cd under conditions that disrupt cellular metabolism. Cadmium accumulated under these altered conditions was then assigned to a specific subcellular local. Results from these experiments suggest that the majority of Cd is accumulated in a metabolism-dependent manner and is localized to the symplasm of root tissues. The remainder is accumulated in a metabolism-independent manner within the apoplasm. The second approach, exemplified by the work of MacRobbie and Dainty (1958), Kochain and Lucas (1982), Rauser (1987), and Blaudez *et al.* (2000), involves desorbing cations from roots following an exposure (loading) period. Data profiles of the cation level remaining in the tissue over the desorption period are dissected into sub-components using non-linear regression techniques (for reviews see Cheesman 1996, Lasat *et al.* 1998). Each component of the curve is suggested to represent a subcellular cation pool, and the size and exchange times for each pool can be derived from the curve. Results using this approach suggest that the apoplasm or cell wall is the largest pool for accumulated divalent cations, followed by the cytoplasm and vacuole. Conclusions made using these different experimental approaches are strikingly different, yet this discrepancy has not been explored in depth. The desorption approach has received criticism based on the assumptions necessary to interpret experimental data. Several authors (Walker and Pitman 1976, MacRobbie 1971) have questioned the assumption that individual compartments (cell wall, cytoplasm, and vacuole) act in a series, and the assumption that a single movement rate between any two compartments must be invoked.

A direct measurement of subcellular Cd location is necessary to understand why differences in results are observed between different experimental approaches. Until direct measurements are obtained, assignments or suggestions of specific subcellular locations for accumulated Cd based on indirect analyses must remain speculative.

1.4 A model system to examine Cd localization at the subcellular level.

In order to directly examine Cd accumulation and localization at the subcellular level, a system is required that allows separation of subcellular compartments while

minimizing the potential for Cd contamination between them. Such a system is now available making use of cells of the giant algae, *Chara corallina*. Surgical techniques that can separate a single cell into cell wall, protoplasm, and vacuolar fractions have been developed for this organism (Reid and Smith 1992, Taylor *et al.* 2000).

Chara corallina is a freshwater algae belonging to the Characeae family. The Characeae are found naturally throughout the world. They inhabit freshwater streams, ponds, and lakes, but can accommodate brackish conditions with up to two-thirds the salinity of sea water (Wood and Imahori 1965). The Characeae are found most commonly in temperate zones, but have been found in the Himalayas and the arctic (Wood and Imahori 1965). They can tolerate varying light levels, occupying shallow beaches as well as lake bottoms with depths reaching 20 m. The general morphology of this family consists of a plant-like form with whorls of single cells separated by long internodal cells (Fig. 1.1). The growth form is plastic and affected by environmental conditions. Undisturbed regions with lower light levels are conducive to development of elongated and diffused plantlets, while higher light levels, brackish water, and/or agitated regions produce a stunted and tufted morphology (Wood and Imahori 1965).

The length of the internodal cells (3-15 cm) and the ease of isolation and manipulation makes *Chara corallina* a model species well suited for use in scientific study. The Characeae have been previously used in studies of ion transport (*Nitellopsis* - MacRobbie and Dainty 1958; *Chara corallina* – Whitington and Bison 1994, Reid *et al.* 1996a&b, Reid and Smith 1992, Taylor *et al.* 2000), membrane permeability (Bisson 1984), and electrophysiology along the length of the internodal cells (Lucas and Smith 1972). This wealth of research work has resulted in the development of a model system that can be utilized to directly examine Cd accumulation and distribution at the subcellular level in a single plant-like cell. Use of single internodal cells avoids complications arising from use of complex tissues (eg. Cataldo *et al.* 1983, Hart *et al.* 1998). The objective of the research presented in this thesis is to directly measure Cd accumulation and localization at the subcellular level and to understand the nature of accumulation in the cell wall, cytoplasm, and vacuole.

1.5 References

Atal, N., Saradhi, P.P., Mohanty, P. 1991. Inhibition of the chloroplast photochemical reactions by treatment of wheat seedlings with low concentrations of cadmium: analysis of electron transport activities and changes in fluorescence yield. Plant Cell Physiol. 32: 943-951.

Alloway, B.J. 1997. Cadmium. *In* Heavy metals in soils. Second edition. Edited by B.J. Alloway. Blackie Academic & Professional. London. pp. 122-151.

Baszynski, T., Wajda, L., Krol, M., Wolinska, D., Krupa, Z., Tukendorf, A. 1980. Photosynthetic activities of cadmium-treated tomato plants. Physiol. Plant. 48: 365-370.

Blaudez, D., Botton, B., Chalot, M. 2000. Cadmium uptake and subcellular compartmentation in the ectomycorrhizal fungus *Paxillus involutus*. Microbiology. 146: 1109-1117.

Bisson, M.A. 1984. Calcium effects on electrogenic pump and passive permeability of the plasma membrane of *Chara corallina*. J. Membrane Biol. 81: 59-67.

Boggess, S.F., Willavize, S., Koeppe, D.E. 1978. Differential response of soybean varieties to soil cadmium. Agronomy Journal. 70: 756-760.

Cataldo, D.A., Garland, T.R., Wildung, R.E. 1983. Cadmium uptake kinetics in intact soybean plants. Plant Physiol. 73: 844-848.

Chaney, R.L., Ryan, J.A., Li, Y.-M., Welch, R.M., Reeves, P.G., Brown, S.L., Green, C.E. 1996. Phyto-availability and bio-availability in risk assessment for cadmium in agricultural environments. *In* OECD Proceedings. Sources of cadmium in the environment. pp. 49-78.

Cheesman, J.M. 1986. Compartmental efflux analysis: an evaluation of the technique and its limitations. Plant Physiol. 80: 1006-1011.

Choudhary, M., Bailey, L.D., Grant, C.A., Leisle, D. 1995. Effect of Zn on the concentrations of Cd and Zn in plant tissue of two durum wheat lines. Can. J. Plant Sci. 75: 445-448.

Clemens, S., Antosiewicz, D.M., Ward, J.M., Schachtman, D.P., Schroeder, J.I. 1998. The plant cDNA *LCT1* mediates the uptake of calcium and cadmium in yeast. Proc. Natl. Acad. Sci. 95: 12043-12048.

Codex Alimentairus Commission. 2000. Report of the thirty-second session of the Codex Committee on Food Additives and Contaminants. Joint FAO/WHO Food Standards Programme, 20-24 March 2000, Beijing, People's Republic of China.

Costa, G., Morel, J.L. 1993. Cadmium uptake by *Lupinus albus* (L.): Cadmium excretion, a possible mechanism of cadmium tolerance. J. Plant Nutr. 16: 1921-1929.

Eklund, M. 1995. Cadmium and lead deposition around a Swedish battery plant as recorded in oak tree rings. J. Environ. Qual. 24: 126-131.

Florjin, P.J., Van Busichem, M.L. 1993. Uptake and distribution of cadmium in maize inbred lines. Plant Soil. 150: 25-32.

Garnham, G.W., Codd, G.A., Gadd, G.M. 1992. Kinetics of uptake and intracellular location of cobalt, manganese and zinc in the estuarine green alga *Chlorella salina*. Appl. Microbiol. Biotechnol. 37: 270-276.

Grant, C.A., Buckley, W.T., Bailey, L.D., Selles, F. 1997. Cadmium accumulation in crops. Can. J. Plant Sci. 78: 1-17.

Hart, B.A., Bertram, P.E., Scaife, B.D. 1979. Cadmium transport by *Chlorella pyrenoidosa*. Environ. Res. 18: 327-335.

Hart, J.J., Welch, R.M., Norvell, W.A., Sullivan, L.A., Kochain, L.V. 1998. Characterization of cadmium binding, uptake, and translocation in intact seedlings of bread and durum wheat cultivars. Plant Physiol. 116: 1413-1420.

Hirschi, K.D., Korenkov, V.D., Wilganowski, N.L., Wagner, G.J. 2000. Expression of Arabidopsis *CAX2* in tobacco. Altered metal accumulation and increased manganese tolerance. Plant. Physiol. 124: 125-133.

Homma, Y., Hirata, H. 1984. Kinetics of cadmium and zinc absorption by rice seedling roots. Soil Sci. Plant. Nutr. 30: 527-532.

Jarvis, S.C., Jones, H.P., Hopper, M.J. 1976. Cadmium uptake from solution by plants and its transport from roots to shoots. Plant Soil. 44: 179-191.

Jones, K.C., Jackson, A., Johnston, A.E. 1992. Evidence for an increase in the cadmium content of herbage since the 1860's. Environ. Sci. Technol. 26: 834-836.

Jolly, W.J. 1984. Modern inorganic chemistry. McGraw-Hill Inc. New York, NY. pp. 61, 281.

Kochain, L.V., Lucas, W.J. 1982. Potassium transport in corn roots. I. Resolution of kinetics into a saturable and linear component. Plant Physiol. 70: 1723-1731.

Lasat, M.M., Baker, A.J.M., Kochain, L.V. 1998. Altered Zn compartmentation in the root symplasm and stimulated Zn absorption into the leaf as mechanisms involved in Zn hyperaccumulation in *Thlaspi caerulescens*. Plant Physiol. 118: 875-883.

Little, P., Martin, M.H. 1972. A survey of zinc, lead, and cadmium in soil and natural vegetation around a smelting complex. Environ. Pollut. 3: 241-254.

Llamas, A., Ullrich, C.I., Sanz, A. 2000. Cd^{2+} effects on transmembrane electrical potential difference, respiration and membrane permeability of rice (*Oryza sativa* L.) roots. Plant and Soil. 219: 21-28.

Lombi, E., Zhao, F.J., McGrath, S.P., Young, S.D., Sacchi, G.A. 2001. Physiological evidence for a high-affinity cadmium transporter highly expressed in a *Thlaspi caerulescens* ecotype. New Phytologist. 149: 53-60.

Lucas, W.J., Smith, F.A., 1972. The formation of alkaline and acid regions at the surface of *Chara corallina* cells. J. Exp. Bot. 78: 1-14.

MacRobbie, E.A.C. 1971. Fluxes and compartmentation in plant cells. Annu. Rev. Plant Physiol. 22: 75-96.

MacRobbie, E.A.C., Dainty, J. 1958. Ion transport in *Nitellopsis obtusa*. J. Gen. Physiol. 42: 335-353.

Malik, D., Sheoran, I.S., Singh, R. 1992. Carbon metabolism in leaves of cadmium treated wheat seedlings. Plant Physiol. Biochem. 30: 223-229.

Nordberg, G. 1996. Human cadmium exposure in the general environment and related health risks – A review. *In* OECD Proceedings. Sources of cadmium in the environment. pp. 95-104.

Rauser, W.E. 1987. Compartmental efflux analysis and removal of extracellular cadmium from roots. Plant Physiol. 85: 62-65.

Reid, R.J., Smith, F.A. 1992. Measurement of calcium fluxes in plants using ^{45}Ca. Planta. 186: 558-566.

Reid, R.J. 1996a. Brookes, J.D., Tester, M.A., Smith, F.A. The mechanism of zinc uptake in plants. Characterization of the low-affinity system. Planta. 198(1): 39-45.

Reid, R.J. 1996b. Rengel, Z., Smith, F.A. Membrane fluxes and comparative toxicities of aluminium, scandium and gallium. J. Exp. Bot. 47: 1881-1888.

Reid, R.J., McLaughlin, M.J., Dunbar, K., Barritt, A.R. 1999. Mechanisms of membrane permeation by trace metals. *In* Proc. 5th Intern. Conf. on the Biogeochem. of Trace Elements; Vienna 1999. pp. 748-749.

Roberts., T.L. 1996. Fertilizer input of cadmium into Canadian Prairie Soils. *In* OECD Proceedings. Fertilizers as a source of cadmium. pp. 136-139.

Ryan, J.A., Pahren, H.R., Lucas, J.B. 1984. Controlling cadmium in the human food chain: A review and rationale based on health effects. Env. Res. 28: 251-302.

Salt, D.E., Wagner, G.J. 1993. Cadmium transport across tonoplast of vesicles from oat roots. Evidence for a Cd^{2+}/H^{+} antiport activity. J. Biol. Chem. 268: 12297-12302.

Taylor, G.J., McDonald-Stephens, J.L., Hunter, D.B., Bertsch, P.M., Elmore, D., Rengel, Z., Reid, R.J. 2000. Direct measurement of aluminum uptake and distribution in single cells of *Chara corallina*. Plant Physiol. 123: 987-996.

Thomine, S., Wang, R., Ward, J.M., Crawford, N.M., Schroeder. J.I. 2000. Cadmium and iron transport by members of a plant metal transporter family in *Arabidopsis* with homology to *Nramp* genes. Proc. Natl. Acad. Sci. 97: 4991-4996.

Walker, N.A., Pitman, M.G. 1976. Measurement of fluxes across membranes. *In* Encyclopedia of Plant Physiology, New Series, Vol. 2A. Edited by U., Luttage, and M.G. Pitman. Springer-Verlag, Berlin. pp. 93-128.

Whittington, J., Bisson, M.A. 1994. Na^{+} fluxes in *Chara* under salt stress. J. Exp. Bot. 45: 657-665.

Wood, R.D., Imahori, K. 1965. A revision of the Characeae. Verlag Von J. Cramer. New York, NY. pp. 1-9.

Table 1.1. Comparison of selected atomic characteristics of potential competitor nutrient cations of cadmium (Jolly 1984).

Ion	Ionic Radius (Å)	Electronegativity
Cd^{2+}	0.97	1.7
Zn^{2+}	0.74	1.6
Fe^{2+}	0.76	1.8
Mn^{2+}	0.80	1.5
Cu^{2+}	0.70	1.9
Mg^{2+}	0.65	1.2
Ca^{2+}	0.99	1.0

Chapter 2. Accumulation and localization of cadmium in internodal cells of *Chara corallina*.

2.1. Introduction

A thorough knowledge of cadmium (Cd) accumulation and localization at the subcellular level is an important step towards understanding the accumulation and localization of Cd at the tissue, organ, and whole plant level. This knowledge can then be used to define further research aimed specifically at reducing Cd accumulation at these larger scales. Due to the small size of plant cells and the lack of suitable micromanipulation techniques, direct measurement of Cd present in the apoplasm (cell wall and extracellular spaces) and symplasm (cytoplasm) has not been achieved. Nonetheless, a large amount of work examining Cd accumulation and localization has been conducted on root tissue, the primary site of Cd exposure in agricultural systems. Previous research has made use of metabolic inhibitors and low temperatures to identify pools of Cd within root tissue. These pools were then assigned to either the apoplasm or symplasm based on assumptions about the nature of Cd accumulation.

In order to critically evaluate previous efforts to measure Cd accumulation and localization, an understanding of the methodologies and assumptions used by various investigators is necessary. Studies conducted with roots of white lupin (Costa and Morel 1993), wheat (Hart *et al.* 1998, Fig. 2.1), and soybean (Cataldo *et al.* 1983, Fig. 2.2) show that rates of Cd accumulation increase rapidly with exposure to increasing concentrations of Cd in the 1-250 nM range. At concentrations above 250 nM, rates increase in a linear fashion. In wheat, this biphasic pattern has been mathematically dissected into a saturable and linear component (Hart *et al.* 1998, Fig. 2.1A). The saturable component has been suggested to be metabolism-dependent, and the linear component metabolism-independent. Accumulation in white lupin (Costa and Morel 1993, data not presented) and soybean (Cataldo *et al.* 1983, Fig. 2.2) was also suggested to have both metabolism-dependent and metabolism-independent components. Two major approaches have been used to alter the metabolic state of root tissue cells and suggest the subcellular location of the metabolism-dependent and metabolism-independent components. Hart *et al.* (1998)

used low temperature treatments while Cataldo *et al.* (1983) used metabolic inhibitors.

Hart *et al.* (1998) partitioned total Cd accumulation in roots of wheat into a metabolism-dependent and metabolism-independent fraction using cold temperature as a method of disrupting metabolism. These authors looked at rates of Cd accumulation at various Cd concentrations in wheat roots exposed to different temperatures (23 °C vs. 2 °C, Fig. 2.1B). At 23 °C, the relationship between rates of Cd accumulation and Cd concentrations in exposure solutions showed a biphasic pattern that could be dissected into a saturable and a linear component. Mathematical analysis of the biphasic accumulation pattern was previously used in the examination of potassium (K^+) accumulation in corn roots (using Rb^+ as a marker, Kochain and Lucas 1982), but stems from work by Epstein in the 1950's (Epstein and Hagan 1952). Both components of the Rb^+ biphasic accumulation curve were interpreted as symplasmic accumulation as very little Rb^+ was suggested to be associated with the cell wall. When viable wheat roots were exposed to Cd at 2 °C, the saturable component of the biphasic curve was almost eliminated (Fig. 2.1B open circles). The authors interpreted this data as being consistent with the inhibition of a metabolism-dependent transport mechanism present at the plasma membrane. Examination of Cd accumulation in methanol/chloroform prepared cell wall fractions resulted in an accumulation pattern similar to that of the predicted linear component at 23 °C (Fig. 2.1B closed squares). This suggested that the linear component of the biphasic pattern in this system was due to Cd accumulation in the cell wall. Rates of accumulation in the purified cell walls were also reduced at 2 °C. The authors suggested that accumulation in the cell wall was 'purely a physical process' (Hart *et al.* 1998). From these analyses, the linear component of Cd accumulation was interpreted as apoplasmic accumulation and the saturable component of Cd accumulation was interpreted as symplasmic accumulation. As an aside, it is interesting to note the differences in interpretation of the linear component of accumulation between the monovalent (Kochain and Lucas 1982) and divalent (Hart *et al.* 1998) cations, despite the similarities in shape of the curve.

Cataldo *et al.* (1983) took a somewhat different approach to identify Cd accumulated in the apoplasm and symplasm. They partitioned total accumulation in

soybean roots into two fractions: readily-exchangeable and absorbed (Fig. 2.2). The readily-exchangeable fraction was defined as the Cd fraction removed by a one minute rinse in 0.5 mM $CaCl_2$, and a 90 minute desorption in $CaCl_2$ plus a 20 fold excess of unlabelled Cd. This fraction was assumed to be Cd bound to readily-exchangeable sites within the apoplasm. Cadmium remaining after these treatments was defined as the absorbed fraction. This absorbed fraction was interpreted to include Cd tightly bound to sites within the apoplasm and Cd within the symplasm. The quantity of Cd in each of these pools was assessed experimentally by monitoring Cd accumulation when roots were exposed to metabolic inhibitors (2,4-dinitrophenol (DNP), sodium azide (NaN_3), or sodium pentobarbitol). Cadmium accumulated in the presence of metabolic inhibitors was termed the non-exchangeable fraction. This fraction was then subtracted from the absorbed fraction and the remainder defined as the metabolically absorbed fraction (Fig. 2.2B). In using this approach, Cataldo *et al.* (1983) did not directly measure the metabolically absorbed fraction. At this point, Cataldo *et al.* (1983) had operationally defined their two Cd fractions, but additional information was required to assign these fractions to specific cellular location.

Cataldo *et al.* (1983) then argued that cation inhibition studies provided information about the nature of Cd accumulation in root tissue that can be used to assign non-exchangeable and metabolically absorbed fractions to apoplasmic or symplasmic locations. Roots were exposed to solutions of radioactive ^{109}Cd and 5-fold excesses of competing cations. These included unlabelled Cd^{2+}, and the nutrient cations Cu^{2+}, Fe^{2+}, Fe^{3+}, Mn^{2+}, and Zn^{2+}. All cations tested reduced total ^{109}Cd accumulation by 25-35%. Root to shoot movement of ^{109}Cd was also reduced by 22-43%, suggesting active transfer from the root symplasm to the xylem. Unlabelled Cd also inhibited accumulation of $^{65}Zn^{2+}$ and $^{54}Mn^{2+}$. Double reciprocal plots of ^{109}Cd accumulation in the presence of either Zn^{2+} or unlabelled Cd^{2+} indicated a competitive inhibitory effect. These observations led the authors to suggest that Cd was accumulated in a metabolism-dependent fashion as an analogue of nutrient cations. This idea was previously suggested by Jarvis *et al.* (1976) during an examination of Cd accumulation in ryegrass. Accumulation of Cd was proposed to be similar to other active mechanisms of nutrient

cation transport, if not by an identical or shared mechanism. Cataldo *et al.* (1983) concluded that the metabolically absorbed (or metabolism-dependent) fraction represented Cd that crossed the plasma membrane (symplasmic accumulation). Accumulation in the presence of metabolic inhibitors (non-exchangeable fraction) was suggested to occur in the cell wall (apoplasm).

In interpreting their data, both groups of authors made the same assumptions. First, all Cd accumulated in the metabolism-dependent fraction was assumed to be localized to the symplasm. In Hart *et al.*'s case (1998), this assumption was explicitly stated, but not tested. In Cataldo *et al.*'s case (1983), this assumption was based upon cation inhibition analysis. A second assumption was that all Cd in the metabolism-independent fraction is present in non-exchangeable sites within the apoplasm. The main problem with these assumptions is that is that neither the apoplasmic nor symplasmic pools were directly measured. Both groups were working with complex tissues and trying to extrapolate their data to a cellular system. Unfortunately, when exposing root tissue to experimental solution, not all root cells are subjected to identical conditions. Cells on the root surface are immediately exposed to Cd while those in the interior of the root have delayed exposure. Similarly during the desorption procedure, exchange of ^{109}Cd from internal cell walls would take longer. This would result in the incorrect assignment of some readily-exchangeable Cd present at internal cell walls to the non-exchangeable component. In addition, some of the basic assumptions of the technique may be incorrect. These assumptions were necessary due to limitations in available measurement techniques, but without a direct measurement of either subcellular pool, the nature and location of the accumulated Cd cannot be conclusively identified. It may be that the apoplasmic pool has a metabolism-dependent component associated with it and the symplasmic pool has a metabolism-independent component. This led me to question the assignments of all metabolism-dependent accumulation as symplasmic Cd and all metabolism-independent accumulation as apoplasmic Cd.

Cadmium in subcellular pools can now be measured and the validity of previous assumptions used to assign location can be directly tested using *Chara corallina* as a

model system. *Chara corallina* is a freshwater alga that grows in a plant like form (herein referred to as a plantlet), with whorls of cells separated by large internodal cells (Fig. 1.1). This system has been widely used study the physiology and permeability of cellular membranes by measuring electrical potential changes in response to cation addition (Keifer and Lucas 1982, Bisson 1984). Ion accumulation studies have been conducted in this system with numerous cations, including Na^+ (Whittington and Bisson 1994), Ca^{2+} (Reid and Smith 1992), Zn^{2+} (Reid *et al.* 1996a), Sc^{2+}, Ga^{3+} (Reid *et al.* 1996b), and Al^{3+} (Taylor *et al.* 2000, Reid *et al.* 1996b). These more recent studies have taken advantage of new techniques for surgical isolation of the cell wall, protoplasm, and vacuole from individual internodal cells following exposure. The ease of manipulation makes *Chara corallina* an ideal model system to directly study the accumulation and subcellular localization of Cd. This system (in contrast to those used in previous studies) also allows examination of ion accumulation at the single cell level.

The objective of the research described in this chapter was to determine subcellular distribution of Cd accumulated in internodal cells of *Chara corallina* and compare the distribution to that reported in tissues of plant roots. This was done using a combination of radioisotope tracer experiments (^{109}Cd) and surgical procedures to isolate distinct cell wall, protoplasm, and vacuole fractions.

2.2. Materials and Methods

2.2.1. Growth and maintenance of *Chara corallina* cultures

Cultures of *Chara corallina* were propagated vegetatively by harvesting single internodal cells and planting them in a mixture of garden sand and soil submerged in distilled water. Plantlets were cultivated to promote maximal elongation of internodal cells by keeping the water level approximately one inch above the tip of growing plantlets. Tanks were maintained in a growth chamber (Environmental Growth Chambers, Ohio) under controlled environmental conditions (22-24 °C, 26 $\mu mol\ m^{-2}\ s^{-1}$, 16 hr day). Tanks were routinely drained, cleaned, and refilled to minimize the presence of contaminants (algae, fungi, bacteria) in the tanks.

Prior to experimentation, single internodal cells (60-100 mm length, ~0.9 mm diameter) were isolated and stored 12-18 hrs in the dark in a solution consisting of 1.0 mM NaCl, 0.5 mM $CaCl_2$, and 0.1 mM K_2SO_4. Storage in the dark provided a post-harvest recuperation period that eliminated the presence of acid and alkaline bands often found along the length of cells (Lucas and Smith 1972). These repetitive, adjacent bands have different pH values (acid ~ pH 5.5; alkaline – pH 8.5 - 9.5), which would make interpretation of data difficult. Individual cells were checked for viability by examining for the presence of cytoplasmic streaming under a microscope immediately before experiments were conducted.

2.2.2. Confirmation of cell viability

In addition to viability tests at the beginning of each experiment (see above), internodal cells of *Chara corallina* were exposed to solutions of unlabeled $CdCl_2$ to ensure viability of cells over both short and long-term experimental periods. Viability of internodal cells (the presence of cytoplasmic streaming) was confirmed through a 4x ocular lens of a compound microscope. Cells (n=11 per concentration tested) were then pretreated in 0.2 mM $CaCl_2$ (as described above) and exposed to experimental solution (110 ml per cell) containing 0.2 mM $CaCl_2$ or 1, 10, 100, or 1000 nM $CdCl_2$ plus 0.2 mM $CaCl_2$. The presence or absence of cytoplasmic streaming was observed at 3, 6, 12, 18, 24, 32, 40, and 48 hour intervals for each concentration. Cells were considered non-viable when cytoplasmic streaming was absent for more than one measurement interval or the highly ordered chloroplast gel layer was disorganized (indicator of cell death). Data were expressed as the proportion cells remaining viable at the time interval.

2.2.3. Exposure conditions and surgical procedures

After the recuperation period, viable cells were mounted in an exposure chamber with three compartments (1 cell per chamber, Fig 2.3). Compartments were sealed from one another using a mixture of silicon release compound and high vacuum grease (Dow Corning) to form a water insoluble barrier around the cell. Cells were then pretreated in 0.2 mM $CaCl_2$ (background solution, necessary to maintain plasma membrane integrity) for 1 to 1.5 hours to allow cells to adjust to experimental conditions. The background

solution in the center compartment was subsequently removed and replaced with an appropriate experimental solution containing 0.2 mM $CaCl_2$ and $CdCl_2$ labeled with ^{109}Cd (24–58 MBq μg^{-1} - constant for a single experiment, $t_{1/2}$ = 462 days). Solution in the end compartments was replaced with fresh background solution to avoid contamination of cell ends with ^{109}Cd. Cells were exposed to experimental solutions in the dark (<0.5 $\mu mol\ m^{-2}\ s^{-1}$) for up to three hours in short experiments, or up to 24 hours in long-term experiments. All solutions were equilibrated to pH 6.0 using KOH or HCl.

Following exposure, subcellular compartments were surgically isolated according to procedures from Reid and Smith (1992) and Taylor *et al.* (2000). Cells were removed from experimental solutions, briefly rinsed in 0.2 mM $CaCl_2$ (2 seconds), blotted lightly, and allowed to air dry for 20-30 seconds to reduce turgor pressure within the cell (minimizing loss of protoplasmic fluid when cell ends are excised). Ends of cells were then excised with a razor blade, exposing the protoplasm. Contamination of the protoplasm by ^{109}Cd present in the cell wall was eliminated since the cell ends at the excision point were not exposed to radiolabeled solution. To remove the protoplasm, a surgical syringe (23 gauge, 1 inch length) was inserted into one end of the cell and water (1-2 ml) flushed through, leaving a clean, clear cell wall sleeve. When the vacuole was to be isolated, an air bubble was first passed through the cell to dislodge the vacuole. Water was then flushed through the cell (as described above) to remove the now avacuolate protoplasm.

2.2.4. Time course of Cd accumulation

Single internodal cells of *Chara corallina* were exposed to single concentrations of Cd for various times to examine the pattern of Cd accumulation and localization. Cells were exposed (as described above) to experimental solutions containing 0.2 mM $CaCl_2$ with 1, 10, or 100 nM $CdCl_2$ radiolabeled with ^{109}Cd. Short term experiments were conducted over 180 minutes with subcellular compartments collected at 15, 30, 45, 60, 90, 120, and 180 minute intervals. For long-term experiments, subcellular compartments were collected at 0.5, 1, 2, 4, 6, 8, 12, 16, 20, and 24 hours intervals. For each time point during both short and long-term experiments, 4 individual cells were exposed to

experimental solution, each in an individual chamber. Results were expressed as moles Cd accumulated per unit surface area exposed with the associated standard error. Data were collected from 3 or 4 cells (allowance for loss of one cell during surgical isolation of subcellular components).

2.2.5. Cadmium accumulation at varying concentrations

Single internodal cells were prepared as above and exposed for 30 minutes to solutions of 0.2 mM $CaCl_2$ with 10, 50, 100, 250, 500, 1000, 1500, or 2000 nM $CdCl_2$ labeled with ^{109}Cd. It was necessary to limit exposure of cells to 30 minutes at concentrations above 100 nM, as saturation of the protoplasm was observed after 60 minutes in initial experiments (see results and discussion). For each concentration tested, 4 cells were exposed to experimental solution, each cell in a single exposure chamber (as described above). Subcellular compartments were collected from each cell following exposure. Results were expressed as moles Cd accumulated per unit surface area exposed per hour with the associated standard error and represent data collected from 3 or 4 individually exposed cells.

2.2.6. Cadmium accumulation in the presence or absence of metabolic inhibitors or the protoplasm

Single internodal cells were prepared as above and exposed to 1 nM $CdCl_2$ with 0.2 mM $CaCl_2$ for three hours in the presence or absence of 100 nM DNP, 10 nM CCCP (m-chloro carbonyl cyanide phenylhydrazine-as per Taylor *et al.* 2000), or a functional protoplasm. Solutions of the metabolic inhibitors were dissolved in 95% ethanol, such that final ethanol concentration in the exposure solution was 0.95% v/v (Taylor *et al.* 2000). An equal amount of ethanol was added to all solutions. Cells lacking a functional protoplasm (ie. pure cell wall sleeves) were surgically prepared prior to $CaCl_2$ pretreatment. Following exposure, subcellular compartments were collected from cells where applicable. Results from individually exposed cells or cell wall sleeves were expressed as moles Cd accumulated per unit surface area exposed with associated standard error. Each data point represents 4 or 5 individually exposed cells, or cell wall sleeves.

2.2.7. Determination of cadmium

All subcellular fractions (cell wall, protoplasm, avacuolate protoplasm, and vacuole) were dried at 70 °C as the presence of water reduces counting efficiency of the isotope (J. McDonald-Stephens, pers. comm.). Radioactive ^{109}Cd was detected by gamma counting (Gamma 4000, Beckman Instruments). The total amount of Cd accumulated in the various fractions was calculated using the ratio of labeled to unlabeled Cd in the exposure solutions. Results were expressed as moles Cd accumulated per unit surface area exposed. When the rate of accumulation was measured, results were expressed as moles Cd accumulated per unit surface area exposed per hour. Surface area was measured based on the assumption that cells are cylindrical in nature. Cell length was estimated as the amount of cell contained in the center (exposure) compartment. Cell diameter was estimated by pressing isolated cell walls until flattened and measuring the cell diameter with a caliper.

2.3. Results and Discussion

2.3.1. Discussion of terminology, surgical isolation procedures, and limitations of comparison

Use of the terms apoplasm and symplasm are not warranted for the *Chara corallina* model system. These terms were coined to represent the continuity between cell walls and extracellular spaces within a tissue (apoplasm), or the interconnected network of cytoplasm within a tissue (by way of the plasmodesmata; symplasm). Surgical techniques used on the single cells in this study allow a direct isolation of subcellular components. These components will be referred to as the cell wall and the protoplasm. The cell wall represents the clear cell wall sleeve that remains after flushing the interior of the cell with water to remove the protoplasm. The protoplasm represents the cytoplasm, vacuole, and nuclear material collected in the water flush step. The avacuolate protoplasm consists of the cytoplasm and nuclear material collected by flushing with water after the vacuole has been expelled by passing an air bubble through the cell. While the terminology used in previous studies and this current work is not entirely comparable, the spatial units I wish to compare as defined by previous authors are. I will compare data previously reported to represent the apoplasm (Hart *et al.* 1998,

Cataldo *et al.* 1983) to cell wall data reported in this study, and data previously reported to represent the symplasm (Hart *et al.* 1998, Cataldo *et al.* 1983) to protoplasmic data reported herein.

The surgical procedure described in the Materials and Methods provides a means of separating single internodal cells into a cell wall, avacuolate protoplasm, and vacuole. However, definitive identification of these pools is not complete until the fates of the tonoplast and the plasma membrane are determined. Efforts to determine the location of these membranes within the various subcellular fractions using enzyme marker analysis were undertaken, but results were inconclusive. Other questions also remain unanswered. The protoplasm of internodal cells can be differentiated into three parts. The first part is a cytoplasmic gel phase on the internal face of the plasma membrane that contains the chloroplasts and does not move (or stream). The second part is a fast streaming cytoplasmic phase containing the remainder of the cytoplasmic and nuclear material. The final part is a tonoplast-enclosed vacuole that comprises the majority of the intracellular space. When air bubbles were passed through the cell during isolation, the liquid collected was clear suggesting it contained the vacuolar sap. I cannot, however, rule out the possibility that the tonoplast and a portion of the fast flowing cytoplasm could have been ejected at the same time. The lack of chloroplasts in this fraction suggests that the gel phase was left behind.

Flushing water through the cell resulted in removal of the gel phase, which might include the fast flowing phase and the tonoplast. The fate of the plasma membrane also remains unknown. If the plasma membrane remained with the cell wall, the avacuolate protoplasm represents only Cd that has crossed the plasma membrane. If the plasma membrane is removed with the protoplasm in the water flush step, Cd on the cell wall face of the plasma membrane could be collected (a potential source of contamination). Given the levels of Cd accumulated by the cell wall versus the intracellular components (see below), Cd bound to the plasma membrane would represent an extremely small component of total accumulation.

As previously stated, the focus of this study is to compare subcellular Cd previously assigned to a specific cellular location (in tissue level experiments) to direct subcellular measurements of Cd from internodal cells of *Chara corallina*. This research will test whether assumptions made at the tissue level regarding Cd accumulation and localization at the subcellular level are valid. As I am using an algal system for this study, care must be taken when comparing these results to previous studies on vascular plants. Charophyte algae, such as *Chara corallina*, are more closely related to land plants through a common ancestor (Graham 1993) than other green algae based on cladistic analysis of structural features, biochemical features (Graham *et al.* 1991), and ribosomal RNA sequences (Chapman and Buchheim 1991). Differences between species surely do exist. Nonetheless, I feel that using *Chara corallina* as a model system provides and important tool to further our understanding of accumulation processes and ion distribution at the subcellular level.

2.3.2. Viability of internodal cells of *Chara corallina* over exposure periods

Internodal cells were exposed to experimental solutions of $CaCl_2$ and $CdCl_2$ in the absence of the radioactive marker to determine whether cells remained viable throughout the time frame of the proposed experiments. The presence of cytoplasmic streaming (viability marker) was assayed at various times following exposure to 1, 10, 100, or 1000 nM $CdCl_2$ plus 0.2 mM $CaCl_2$, and the proportion of cells remaining viable at times during the exposure period was determined (Fig. 2.4). The first effect of $CdCl_2$ exposure on cellular viability was observed after 18 hours of exposure to 100 nM and 1000 nM $CdCl_2$, where 91% of cells remained viable. This time point was well beyond any exposure time used for experiments at high concentrations. After 48 hours, only 36% of cells at 1000 nM, 55% at 100 nM, and 73% of cells at 10 nM $CdCl_2$ exposure remained viable. Exposure to $CaCl_2$ alone or with 1 nM $CdCl_2$ for 48 hours had no detectible effects on cytoplasmic streaming. These results suggest that internodal cells were viable over the times and concentrations used in this study. The results also show that protoplasmic accumulation is not the result of diffusion across the plasma membranes of dead cells.

2.3.3. Cadmium accumulation and localization over time

Exposure of single internodal cells of *Chara corallina* to Cd resulted in a different pattern of localization than was expected based on results of previous studies. The cell wall of *Chara corallina* was the dominant point of Cd localization, accumulating between 85 and 97 % of total Cd over three hours depending on the exposure concentration (Fig. 2.5 A, B, C). This percentage increased from 85% after 3 hours to approximately 98% of total accumulated Cd after 24 hours of exposure to 1 nM $CdCl_2$ (Fig. 2.6). These values are higher than the 30–50 % reported to accumulate in the apoplasm of roots of soybean (Cataldo *et al.* 1983) and wheat (Hart *et al.* 1998). The rate of accumulation of Cd within the cell wall of *Chara corallina* was observed to decrease over time (Table 2.1). During the first 30 minutes, the accumulation rate was 3.2–9.5 fold higher than the accumulation rate over the remainder of the exposure period (Table 2.1). When the concentration of Cd in the absorption solution was increased, the accumulation rate during the rapid phase (0-30 min) increased 27 fold (10 nM exposure) or 131 fold (100 nM exposure) above the accumulation rate observed during 1 nM exposure conditions. An increase in accumulation rate over the remainder to the exposure period (30-180 min) was also observed and was 9 fold (10 nM exposure) or 116 fold (100 nM exposure) higher than that under 1 nM exposure conditions. Throughout all time-dependent accumulation studies, complete saturation of the cell wall component was not observed agreeing with previous results concerning cell wall accumulation of Cd. However, the amount of Cd accumulated in cell walls of internodal cells of *Chara corallina* represents a larger proportion (~80% more) of total accumulation than previously reported (100 nM exposure, Cataldo *et al.* 1983, Hart *et al.*1998).

The presence of Cd within the protoplasm (both the avacuolate protoplasm and the vacuole) was detectible after 30 minutes with exposure to 1 nM $CdCl_2$ (Fig. 2.7A), and after 15 minutes with exposure to 10 nM $CdCl_2$ (Fig. 2.7C). The rate of accumulation in the total protoplasm was constant over the entire exposure period at both 1nM (Fig. 2.5D, Fig. 2.6) and 10 nM (Fig. 2.5E) exposure conditions, and over 45 minutes at 100 nM exposure (Fig. 2.5F). The rate of accumulation increased 3.4 fold (10 nM exposure) or 65 fold (100 nM, 60 minutes) above the rate observed under the 1 nM

exposure condition (Table 2.1). These results agreed with previous research insofar as they suggest that the symplasm/protoplasm and vacuole of plant cells is accessible to Cd (Salt and Wagner 1993). Again, however, differences were observed between this study and previous work with respect to the degree of accessibility. In my work, accumulation of Cd in the protoplasm of internodal cells accounted for as much as 15% (1 nM exposure, Fig. 2.5D) and as little as 3% (100 nM exposure, Fig. 2.5F) of total Cd. Saturation of the protoplasm was observed after 60-90 minutes with exposure to 100 nM $CdCl_2$ (Fig. 2.5F). This saturation was not observed in both short and longer exposure to low concentrations (Fig. 2.5D, Fig. 2.6). The observed saturation can be explained by the fact the single cells have a finite protoplasmic volume, which may have reached its capacity to accumulate Cd under the 100 nM exposure conditions. Protoplasmic accumulation of Cd (3-15% of total) in internodal cells of *Chara corallina* contrasts with the reported symplasmic accumulation of 50–70% of total Cd from tissue studies (Cataldo *et al.* 1983, Hart *et al.* 1998). If we accept that studies are indeed measuring what they claim to measure, this would suggest that the protoplasm of internodal cells is less accessible than the symplasm of the root tissues examined.

Accumulation of Cd in the protoplasm of internodal cells of *Chara corallina* was equally divided between the avacuolate protoplasm and the vacuole over longer periods of exposure to 1 nM $CdCl_2$ (Fig. 2.7B). The vacuole has been previously suggested to be a major compartment of Cd accumulation in plants (Salt and Wagner 1993), potentially acting in sequestration (reducing long range transport in a plant) and detoxification of harmful metal ions. Beyond the conclusion that the vacuole is accessible to Cd, the data presented here neither agree nor disagree with these potential roles. Accumulation of Cd as a sequestration mechanism could not be explored with these experiments, as movement of Cd from the single internodal cell was not examined. However, accumulation of half the protoplasmic Cd in the vacuole would reduce the amount of Cd available for remobilization throughout the plantlet. As all cells on a plantlet would be exposed to similar conditions in the natural environment, mobilization of ions between *Chara corallina* cells may not be important. The vacuole could also act as a cation storage system not specific to Cd. This system could either store necessary cations until

low environmental concentrations are encountered, or detoxify potentially harmful substances by limiting their access to the protoplasm.

2.3.4. Kinetic investigation of cadmium accumulation

An investigation of the rate of Cd accumulation in internodal cells of *Chara corallina* over a range of concentrations similar to those used in tissue studies (Cataldo *et al.* 1983, Costa and Morel 1993, Hart *et al.* 1998) showed some similarities between the systems, but still reflected the large accumulation potential of the cell wall (Fig. 2.8). The rate of accumulation in the cell wall increased linearly with respect to exposure concentrations up to 2000 nM $CdCl_2$ (Fig 2.8A). This agrees with work in wheat (Fig. 2.1, Hart *et al.* 1998) where the subtracted linear component was suggested to be accumulation in the cell wall, and soybean (Fig. 2.2A, Cataldo *et al.* 1983) where the non-exchangeable component was linear with exposure up to 2000 nM $CdCl_2$. In both of these studies, however, the symplasm was suggested to be the dominant location for accumulated Cd. The opposite was observed in *Chara corallina*. Over the range of Cd concentrations examined, the protoplasm accumulated at most 15% of total Cd, and this value decreased with increasing concentration (Fig. 2.5, Fig. 2.8).

Previous research had proposed that the saturable portion of the accumulation rate versus exposure concentration plot was due to active transport across the plasma membrane. Data from the saturable component were fit to a Michaelis-Menton model, and K_m and V_{max} values were calculated (see Fig. 2.1 for example). The same model was applied to the protoplasmic data obtained in this study (Table 2.2). The calculated V_{max} values for transport into the total and avacuolate protoplasm were off the scale of the graph (Fig. 2.8B), indicating that concentrations at the plasma membrane had not yet saturated the Cd 'carrier'. The V_{max} value for the vacuole was within the bounds of the graph (Fig 2.8B, Table 2.2), but also had not yet been reached. The K_m values for the total and avacuolate protoplasm were also off the graph scale (Fig. 2.8B). Accumulation rates at higher concentrations need to be obtained in order to evaluate the validity of the calculated constants. The fact that V_{max} and K_m values for the avacuolate protoplasm were higher than the total protoplasm values was initially puzzling. However, the high

standard error and P-values associated with these constants suggests they are not reliable estimates of the true values in this compartment. Analysis of accumulation within the protoplasm is complicated by the fact that the cell wall is such a large pool of Cd accumulation. Over the 30 minute exposure period under 2000 nM conditions, 99.4% of total Cd was accumulated in the cell wall (Fig. 2.8). It is possible the plasma membrane experienced a different Cd concentration than present in the exposure solution. Cadmium levels at the plasma membrane may not yet saturate the proposed active transport mechanism.

2.3.5. Accumulation of cadmium under altered metabolic conditions

Previous assignment of Cd to a specific cellular location was based on Cd accumulation under altered metabolic conditions (Cataldo *et al.* 1983, Hart *et al.* 1998). All Cd accumulated in a metabolism-dependent manner was suggested to be symplasmic and all metabolism-independent accumulation was apoplasmic. Cadmium accumulation in the presence of the metabolic inhibitors DNP and CCCP, and low temperatures was conducted as a direct test of these assumptions. With the surgical techniques available, Cd accumulation in the absence of a functional protoplasm was also conducted. This experiment provided powerful test of the second assumption, that all Cd accumulated in the apoplasm was a result of metabolism-independent processes. If this assumption is valid, accumulation in cell walls of intact and pre-exposure isolated cell walls should be equal.

It should be noted that experiments altering cellular metabolism (by metabolic inhibitor or low temperature exposure) were not designed to pinpoint a specific aspect of cellular metabolism responsible for Cd accumulation. Rather, these treatments were used as a general test of the role metabolism can play in accumulation. Data collected from metabolic inhibitor experiments must be interpreted carefully. For example, the inhibitor DNP is known to have numerous effects including uncoupling oxidative phosphorylation, impairing plasma membrane structure and function, and disrupting the proton gradient across the plasma membrane (Jackson 1982). The inhibitor CCCP can uncouple oxidative phosphorylation in mitochondria and chloroplasts (Heytler 1962). Also low temperatures

cause a general reduction in cellular processes and metabolism. Conclusions drawn from these tests should therefore remain general.

Cadmium accumulation in the cell wall when exposed to 1 nM $CdCl_2$ was not significantly reduced by exposure in the presence of metabolic inhibitors (Table 2.3). Exposure in conjunction with low temperatures resulted in a significant reduction (33%) in Cd accumulation. When cell walls isolated before Cd exposure (no protoplasm) were subsequently exposed to Cd, a similar reduction in accumulation (33%) was observed when compared to cell walls of intact cells (Table 2.3). A time course of Cd accumulation in intact and pre- exposure isolated cell walls provided similar results (Fig. 2.9). These results suggest that Cd accumulation by the cell wall of internodal cells occurs via both metabolism-independent (temperature dependent decrease in accumulation of isolated cell walls, Table 2.3) and protoplasm-dependent processes (decrease in accumulation in the absence of a protoplasm and under low temperature treatment, Table 2.3).

Accumulation of Cd in the total protoplasm and its components appeared metabolism-dependent. This agreed with previous assumptions regarding symplasmic accumulation in plants. A reduction of up to 90% was observed (Table 2.3), but differences were not significant. The large standard error associated with the values appeared responsible for the lack of significance between the differences as the collected data approached the detection limits.

Exposure of cells to metabolic inhibitors included exposure to 0.95% ethanol (v/v), as ethanol was necessary to dissolve both inhibitors. Exposing internodal cells to this concentration of ethanol had previously resulted in no adverse effects on cytoplasmic streaming or chloroplast organization (Reid *et al.* 1996b), suggesting cellular viability was not affected. Also, accumulation of Cd in the cell wall and protoplasm of control cells (Table 2.3) was similar to Cd levels accumulated in the absence of ethanol (Fig 2.5A, Fig 2.6), further suggesting that viability was not affected.

Three plausible explanations can be suggested to account for the large discrepancy in specific Cd localization found in this research compared to previous studies. First, I could be observing an accumulation pattern specific to *Chara corallina*, and potentially other green algal species. A study conducted on the chlorophyte alga *Chlamydomonas reinhardtii* demonstrated that algal cell walls have a very large metal ion binding capacity (Button and Hostetter 1977). The abundance of metal binding sites could serve to trap trace metals or cations, increasing the local concentration around the algal cell. This would increase the levels of these substances at the plasma membrane, raising the potential for movement into the protoplasm. Conversely, the cell wall could act as a filter, trapping harmful molecules and restricting their access to the plasma membrane, and the protoplasm. This was suggested by additional work with *Chlamydomonas reinhardtii* showing a decreased survival rate of a mutant strain lacking a functional cell wall compared to wild type cells when exposed to the divalent metal ions Cd^{2+}, Cu^{2+}, Co^{2+}, and Ni^{2+} (Macfie *et al.* 1994). Also, a large Cd fraction was removable from cell walls of this algae when compared to the wall-less mutant strain (Macfie and Welbourn 2000). It can be speculated that both mechanisms are active to different extents.

The second explanation for differences between results is that previous assumptions regarding Cd accumulation and the resulting assignment of absorbed Cd to a specific location are not entirely valid. The presence of a protoplasm-dependent component associated with accumulation in the cell wall directly challenges one of the underlying assumptions regarding assignment of Cd location in plant tissues. This possibility has been previously suggested in work with aluminum (Zhang and Taylor 1991), where a portion of the saturable (and previously presumed symplasmic) component of accumulation was attributed to the cell wall. If a protoplasm-dependent component is associated with cell wall accumulation in plant tissues, previous positional interpretations would be incorrect, and results may more closely resemble accumulation profiles from this study.

The third explanation for the differences observed is that the surgical techniques available with *Chara corallina* internodal cells offer a level of spatial resolution that cannot be realized when working with root tissues. Cadmium accumulation in each distinct subcellular compartment of *Chara corallina* cells can be directly assessed. Due to the indirect nature of the previous analyses, it is not possible to conclusively identify the location of Cd in collected pools when roots were exposed to either the metabolic inhibitor or low temperature treatments. It remains possible that data collected at the tissue level does not accurately reflect processes occurring in one single cell. Instead, the results would represent the average accumulation potential of all cells within the tissue. Not all cells in a given tissue are identical. The root is composed of numerous cell types (for example epidermal, cortex, and vascular cells), each of which has a distinct role within the tissue. In addition to intercellular differences, not all cells are exposed to identical conditions. It may not be valid to assume that a cortex cell would have the same accumulation potential as an epidermal cell, or that accumulation in both cell types occurs in the same manner. Cortex cells are not exposed to the external environment. They can obtain ions from the apoplasm or from neighboring cells via plasmodesmata. The data collected from root tissue would then represent the average accumulation potential for numerous cell types. Specific Cd location in any one cell type could not then be conclusively determined.

The question, "what cell type, if any, would a *Chara corallina* internodal cell be analogous to?" is an interesting point to address. Given the differences between species, an analogy may not be applicable. Both vascular plant and charophyte cells have a cell wall and a plasma membrane that Cd must cross to gain access to the protoplasm, and a tonoplast separating the vacuole from the rest of the cell. The charophyte algae are suggested to have the most recent common ancestor to land plants (Chapman and Buchheim 1991, Graham 1993), suggesting generalities in cellular composition. Beyond these points however, a direct comparison between an internodal cell of *Chara corallina* and a single cell from a plant may not be feasible. This lack of direct cellular comparison should not preclude a re-examination of previously reported data. Data from my direct assessment of Cd localization indicate that Cd is capable of crossing both the plasma

membrane and the tonoplast of a biological system. This was previously suggested from analysis in plant tissue (Cataldo *et al.* 1983, Hart *et al.* 1998, Salt and Wagner 1993). However, with the exception of *in vitro* accumulation in vacuolar protoplasts of oat roots (Salt and Wagner 1993), transport of Cd across the tonoplast was never directly assessed or quantified. The results of my work also question the degree to which the protoplasm is accessible by Cd, as a reduced percentage (3-15%) of total accumulation was observed when compared to previous studies (50-70%). A direct measure of Cd accumulated subcellular locations within plant cells is still necessary to explore the suggestions raised by this study.

A final point that remains to be considered is the physical site(s) to which Cd ions might bind within the cell wall. This point could be addressed by examining the ultrastructure of a Characean cell wall, studies specific to the Characeae are lacking. In lieu of direct knowledge of *Chara corallina* cell wall structure, the general composition of a plant cell wall can provide insights as to the nature of Cd binding within a cell wall.

The plant cell wall is an complex structure that has been described as containing three structurally independent, but interacting, domains (Carpita and Gibeaut 1993). The first domain is comprised of a cellulose microfibril lattice [(1→4) β-linked D-glucose polymers] supported by interlocking glycan polymers. These molecules provide a structural framework. The second cell wall domain is a 'jelly-like' pectin domain, which the cellulose-glycan domain is embedded in. Pectins are complex polysaccharides that are thought to determine many properties of the cell wall, flexibility, porosity, surface charge, cell wall pH, ion balance, and binding capabilities (Carpita and Gibeaut 1993). The third domain consists of various proteins with structural and/or functional properties. Cation binding sites contributed by all three domains comprise the cation binding capacity of the cell wall as a whole.

Based on the structure of the cell wall, possible explanations for the decrease in Cd accumulation observed for isolated cell walls compared with an intact cell walls (Table 2.3, Fig 2.9) wall can be proposed. The pectin matrix is thought to provide most

binding sites for cation accumulation in the cell wall. Deposition of new cell wall material, including pectins, occurs during the exposure period. This would provide new binding sites for Cd, increasing accumulation of Cd in intact cell walls relative to isolated cell walls (with fixed number of binding sites). However, deposition of sufficient material to increase the Cd binding capacity by 33% (Table 2.3) would be unlikely over a three hour exposure. A second possible explanation is that changes in the number of binding sites within the cell wall occurs in intact cells due to the exudation and activity of proteins. A decrease in the methylation status of the pectin matrix (via pectin methylesterase activity) has been suggested to provide binding sites for Ca^{2+}, increasing crosslinking between pectin polymers and condensing the pectin matrix (Carpita and Gibeaut 1993). By removing methyl groups from pectins in the cell wall, more Cd binding sites could potentially become available. This would again increase the Cd accumulation potential in the cell wall of an intact cell over that of an isolated cell wall. The ability to synthesize the enzymes responsible for this activity and provide metabolic energy for their activity is not possible in an isolated cell wall fraction.

While the pectin matrix is thought to contribute the majority of cation binding sites, the potential for binding to the cellulose-glycan lattice should not be ignored. This domain may provide sites for passive binding of cations and contribute to a portion of the Cd accumulation observed in isolated cell wall fractions. A detailed analysis of the cell wall components, their relative distribution, and the rate of cell wall synthesis and protein activity are necessary to fully understand Cd binding within this extremely large subcellular pool.

2.4. Conclusions

The inability to unambiguously separate Cd accumulated at the tissue level into distinct apoplastic and symplastic compartments has hindered a complete and thorough analysis of Cd accumulation in root tissues. Use of *Chara corallina* internodal cells as a model system provided me with an opportunity to directly measure the amount of Cd present in distinct subcellular compartments (cell wall and protoplasm) upon exposure. My results clearly indicate that the cell wall is the major accumulation site for Cd in

internodal cells of *Chara corallina*. The rate of Cd accumulation in the cell wall does not saturate with respect to time or concentration up to 2000 nM $CdCl_2$. Accumulation in the cell wall is not affected by exposure to the metabolic inhibitors DNP or CCCP, but is reduced by exposure to low temperatures or removal of the protoplasm. The protoplasm is accessible to Cd, but to a much lesser extent than the cell wall and shows no saturation in accumulation rate up to 2000 nM $CdCl_2$ over a 30 minute exposure period. However, time dependent saturation is observed after 60 – 90 minutes at 100 nM $CdCl_2$. It is possible that due to the fixed volume of the internodal cells, protoplasmic saturation is reached at this time at higher concentrations. Cadmium accumulation in the total protoplasm and its components appeared metabolism-dependent. Vacuolar accumulation also mirrors accumulation in the avacuolate protoplasm under low exposure concentrations.

Differences between my data and those from previous studies raise questions about the interpretation of earlier results. Subcellular Cd location was assigned to specific subcellular pools based on changes in accumulation in response to an altered metabolic state of the tissue. In this study, Cd accumulation in the cell wall was suggested to occur by both metabolism-independent and protoplasm-dependent processes. This challenges one of the primary assumptions from previous studies (Cataldo *et al.* 1983, Hart *et al.* 1998) that all cell wall accumulation occurred in a metabolism-independent manner. It is possible that previous assumptions regarding metabolic status and cellular localization were not valid. This would have led to misinterpretation and incorrect subcellular assignment of the collected Cd pools. At the time, these assumptions were necessary to interpret previous research. However, with the surgical techniques used in this study, a direct analysis of subcellular Cd distribution was possible. This data shows a much different pattern than previously observed and suggests a re-examination may be warranted.

2.5. References

Bisson, M.A. 1984. Calcium effects on electrogenic pump and passive permeability of the plasma membrane of *Chara corallina*. J. Membrane Biol. 81: 59-67.

Button and Hostetter, 1977. Copper sorption and release by *Cyclotella meneghiniana* (Bacillariophyceae) and *Chlamydomonas reinhardtii* (Chlorophyceae). J. Phycol. 13: 198-202.

Carpita, N.C., Gibeaut, D.M. 1993. Structural models of the primary cell walls of flowering plants: consistency of molecular structure with the physical properties of the walls during growth. Plant J. 3: 1-30.

Cataldo, D.A., Garland, T.R., Wildung, R.E. 1983. Cadmium uptake kinetics in intact soybean plants. Plant Physiol. 73: 844-848.

Chapman, R.L., Buchheim, M.A. 1991. Ribosomal RNA gene sequences: analysis and significance in the phylogeny and taxonomy of green algae. Crit. Rev. Plant Sci. 10: 343-368.

Costa, G., Morel, J.L. 1993. Cadmium uptake by *Lupinus albus* (L.): Cadmium excretion, a possible mechanism of cadmium tolerance. J. Plant Nutr. 16: 1921-1929.

Epstein, E., Hagen, C.E. 1952. A kinetic study of the absorption of alkali cations by barley roots. Plant Physiol. 27: 57-474.

Graham, L.E., Delwiche, C.F., Mishler, B.D. 1991. Phylogenetic connections between the 'green algae' and the 'bryophytes'. Advances in Bryology. 4: 213-244.

Graham, L.E. 1993. The Charophycean algae. *In* The origin of land plants. John Wiley & Sons Inc. N.Y. pp. 56-84.

Hart, J.J., Welch, R.M., Norvell, W.A., Sullivan, L.A., Kochain, L.V. 1998. Characterization of cadmium binding, uptake, and translocation in intact seedlings of bread and durum wheat cultivars. Plant Physiol. 116: 1413-1420.

Heytler, P.G. 1962. Uncoupling of oxidative phosphorylation by carbonyl cyanide phenylhydrazines. I. Some characteristics of m-Cl-CCP action on mitochondria and chloroplasts. Biochemistry. 2: 357-361.

Jackson, P.C. 1982. differences between effects of undissociated and anionic 2,4-dinitrophenol on permeability of barley roots. Plant Physiol. 70: 1373-1379.

Jarvis, S.C., Jones, H.P., Hopper, M.J., 1976. Cadmium uptake from solution by plants and its transport from roots to shoots. Plant Soil. 44: 179-191.

Keifer, D.W., Lucas, W.J. 1982. Potassium channels in *Chara corallina*. Control and interaction with the electrogenic H^+ hydrogen pump. Plant Physiol. 67: 781-788.

Kochain, L.V., Lucas, W.J. 1982. Potassium transport in corn roots. I. Resolution of kinetics into a saturable and linear component. Plant Physiol. 70: 1723-1731.

Lucas, W.J., Smith, F.A., 1972. The formation of alkaline and acid regions at the surface of *Chara corallina* cells. J. Exp. Bot. 78: 1-14.

Macfie, S.M., Tarmohamed, Y., Welbourn, P.M. 1994. Effects of cadmium, cobalt, copper, and nickel on the growth of the green alga *Chlamydomonas reinhardtii*: the influences of the cell wall and pH. Arch. Environ. Contam. Toxicol. 27: 454-458.

Macfie, S.M., Welbourn, P.M. 2000. The cell wall as a barrier to uptake of metal ions in the unicellular green alga *Chlamydomonas reinhardtii* (Chlorophyceae). Arch. Environ. Contam. Toxicol. 39: 413-419.

Reid, R.J., Smith, F.A. 1992. Measurement of calcium fluxes in plants using ^{45}Ca. Planta. 186: 558-566.

Reid, R.J. 1996a. Brookes, J.D., Tester, M.A., Smith, F.A. The mechanism of zinc uptake in plants. Characterization of the low-affinity system. Planta. 198(1): 39-45.

Reid, R.J. 1996b. Rengel, Z., Smith, F.A. Membrane fluxes and comparative toxicities of aluminium, scandium and gallium. J. Exp. Bot. 47: 1881-1888.

Salt, D.E., Wagner, G.J. 1993. Cadmium transport across tonoplast of vesicles from oat roots. Evidence for a Cd^{2+}/H^+ antiport activity. J. Biol. Chem. 47: 1881-1888.

Taylor, G.J., McDonald-Stephens, J.L., Hunter, D.B., Bertsch, P.M., Elmore, D., Rengel, Z., Reid, R.J. 2000. Direct measurement of aluminum uptake and distribution in single cells of *Chara corallina*. Plant Physiol. 123: 987-996.

Whittington, J., Bisson, M.A. 1994. Na^+ fluxes in *Chara* under salt stress. J. Exp. Bot. 45: 657-665.

Zhang, G., Taylor, G.J. 1991. Effects of biological inhibitors on kinetics of aluminium uptake by excised roots and purified cell wall material of aluminium-tolerant and aluminium-sensitive cultivars of *Triticum aestivum* L. J. Plant Physiol. 138: 553-539.

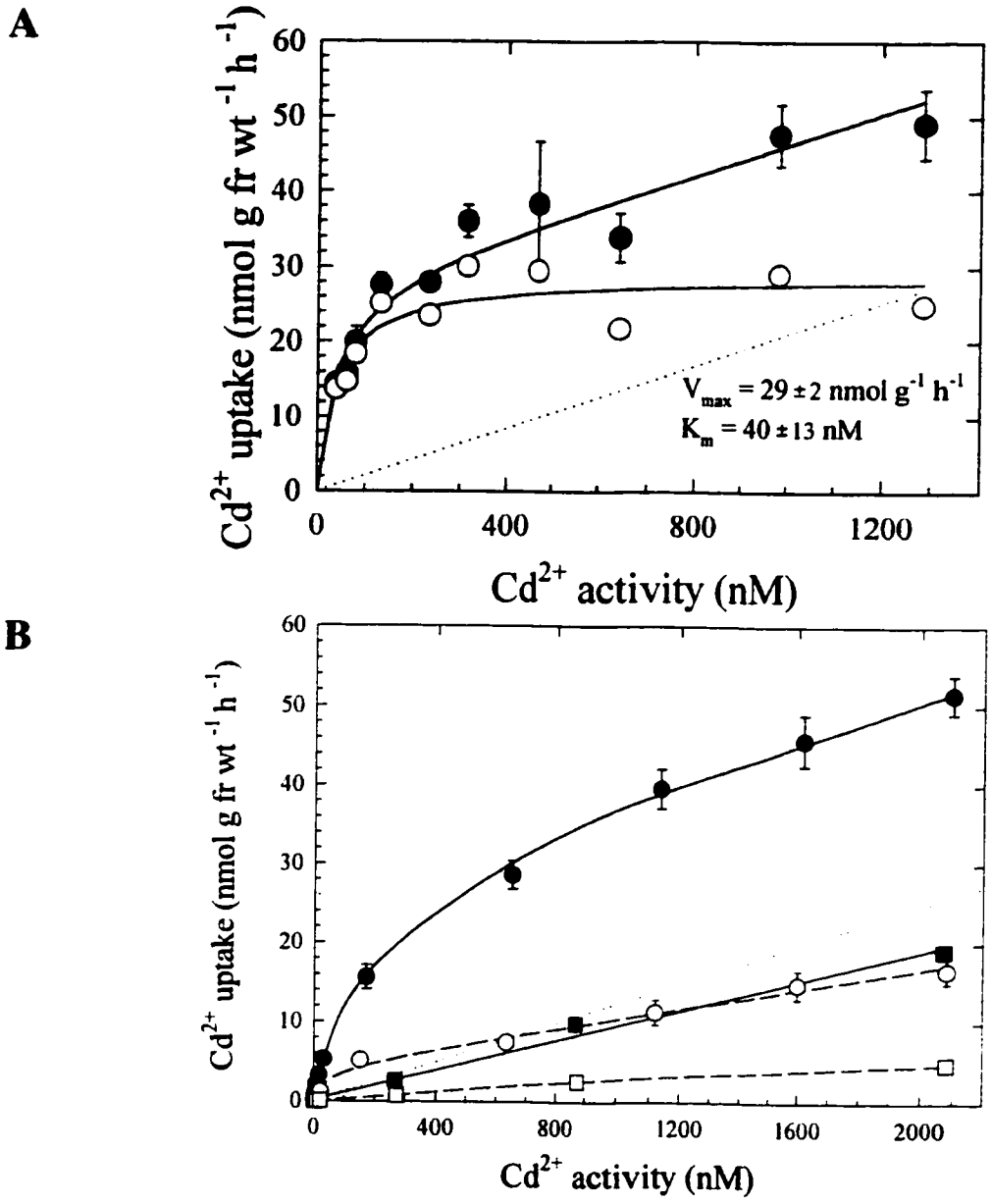

Figure 2.1. The effect of cadmium concentration on the rate of cadmium accumulation in roots of wheat (*Tritium aestivum*). **(A)** Changes in the rate of Cd accumulation in roots (closed symbols) can be mathematically dissected into a saturable (open symbols, V_{max} = 29 ± 2 nmol g^{-1} h^{-1}, K_m = 40 ± 13 nM) and a linear component (dotted line). **(B)** Accumulation of Cd in intact root tissue (circles) and pure cell wall fractions (squares). Closed symbols represent experiments conducted at 23 °C, open symbols are at 2 °C. Dotted line represents linear component of accumulation. Data are taken from Hart *et al.* (1998).

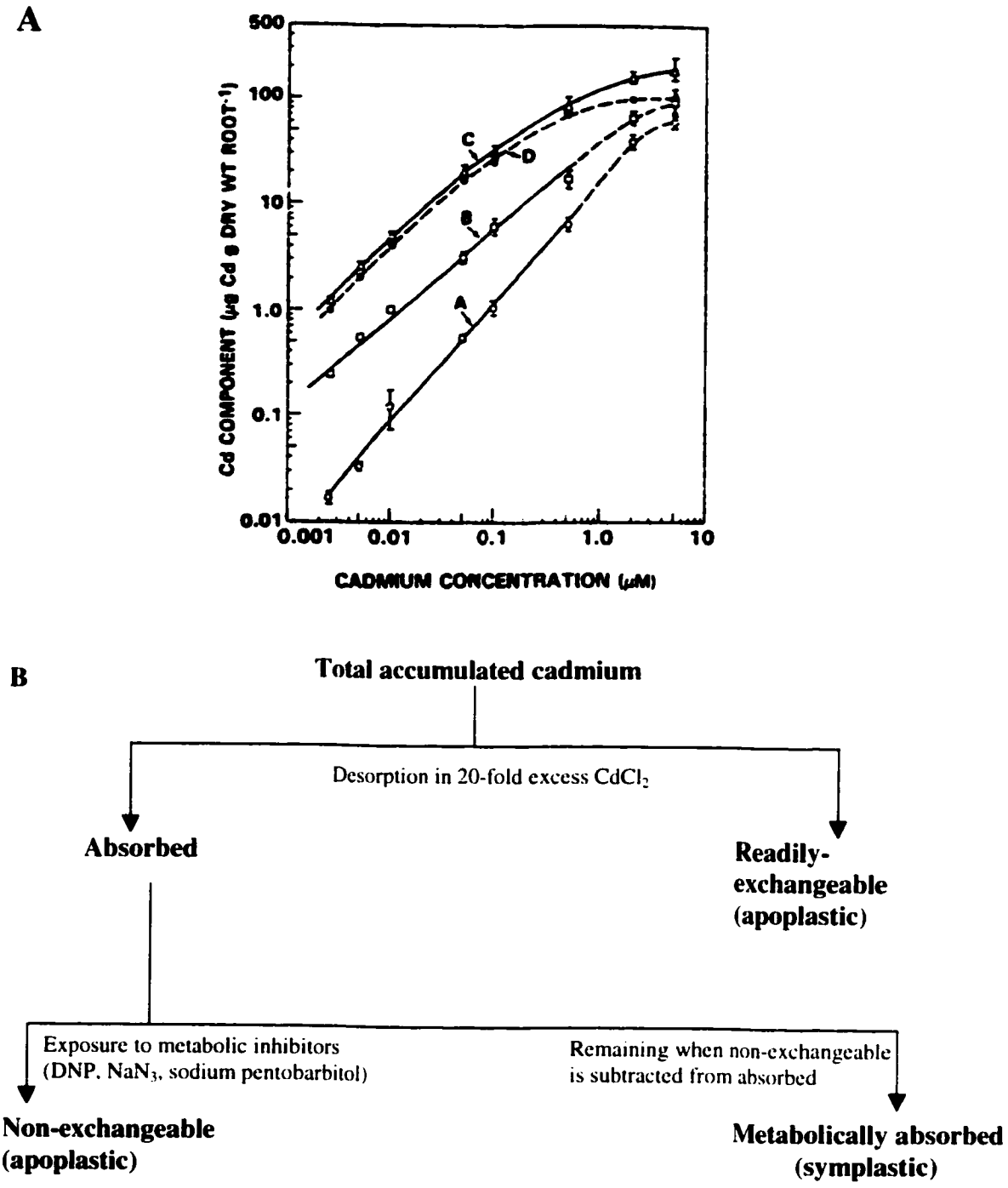

Figure 2.2. Cadmium accumulation in roots of soybean. **(A)** Operationally defined fractions collected from soybean including (a) readily-exchangeable, (b) non-exchangeable, (c) absorbed, and (d) metabolically absorbed. **(B)** Procedural schematic of collection techniques with interpreted subcellular locations. Data from Cataldo *et al.* (1983).

Figure 2.3. An exposure chamber with a single *Chara corallina* internodal cell. Single cells were placed in the three-compartment chamber and the compartments sealed using a mixture of silicon release compound and high vacuum grease to form a water insoluble barrier. For treatment, experimental solution (radioactive) was placed in the centre compartment while the end compartments contained background solution. Contamination of the cell ends was eliminated such that surgery did not introduce ^{109}Cd accumulated by the cell wall to the protoplasm.

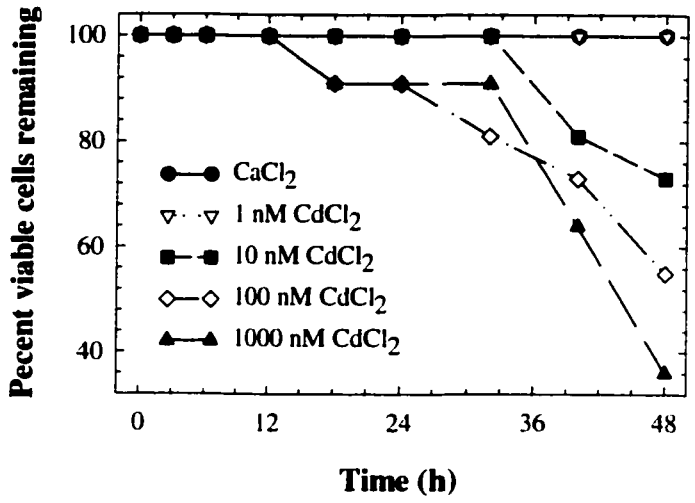

Figure 2.4. Viability of internodal cells of *Chara corallina* over time. Internodal cells of *Chara corallina* were exposed to solutions of $CdCl_2$ + 0.2 mM $CaCl_2$ for up to 48 hours. Cells that showed no cytoplasmic streaming for two consecutive time points, or had a disorganized chloroplast layer were considered to have lost viability. Eleven individual internodal cells were exposed to each concentration.

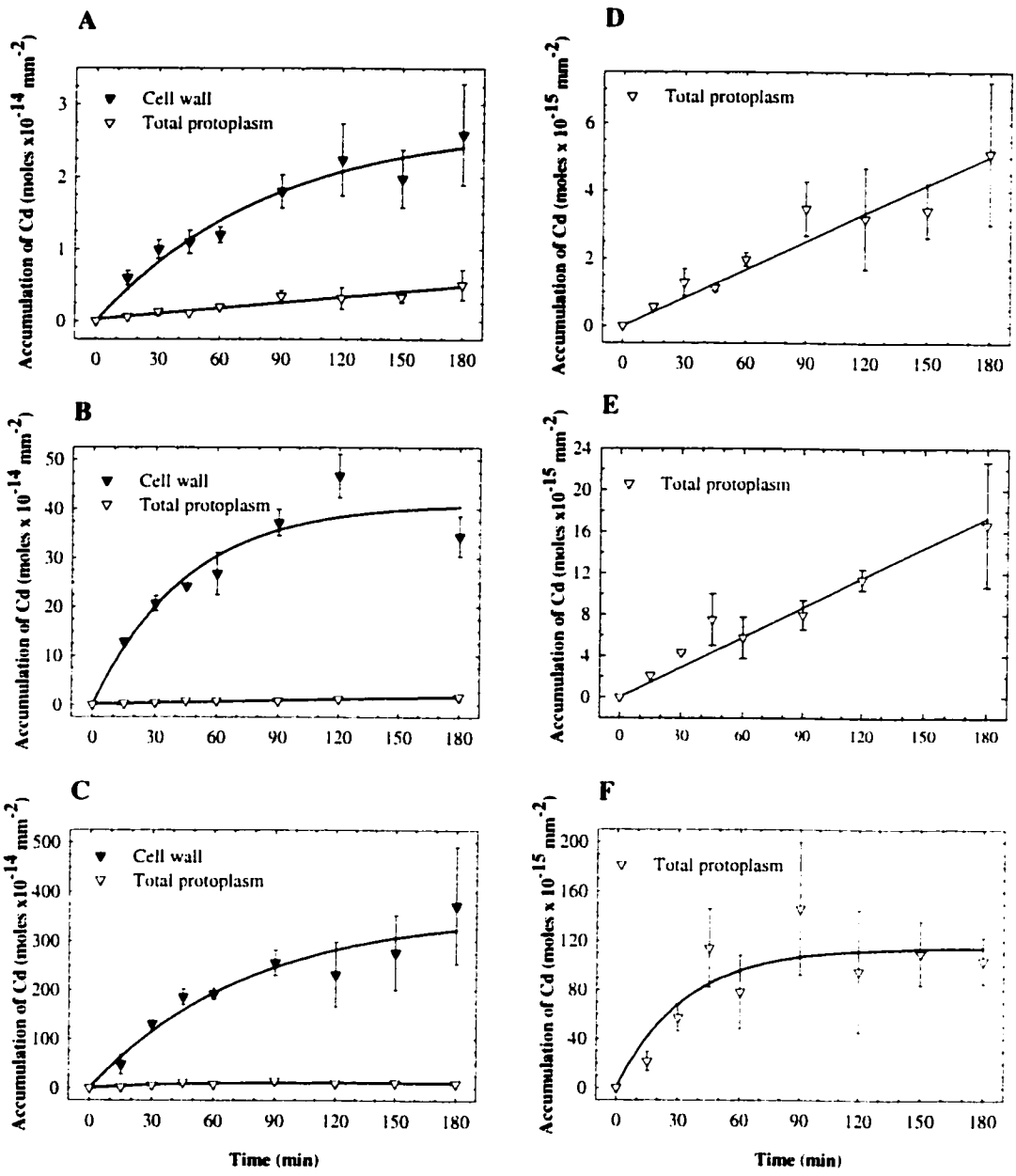

Figure 2.5. Subcellular localization of cadmium in internodal cells of *Chara corallina*. Individual internodal cells were exposed to radiolabeled solutions of $CdCl_2$ + 0.2 mM $CaCl_2$. Subcellular components were surgically isolated at the indicated time points. Exposure concentrations were as follows: (**A**, **D**) 1 nM, (**B**, **E**) 10 nM, (**C**, **F**) 100 nM. Each point represents the mean and standard error of 3 or 4 individually exposed cells.

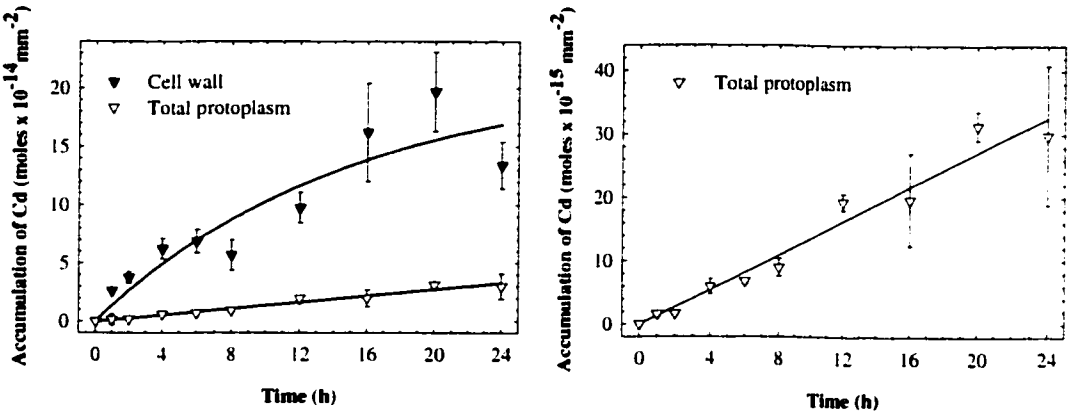

Figure 2.6. Subcellular localization of cadmium over long-term exposure. Individual internodal cells of *Chara corallina* were exposed to a radiolabeled solution of 1 nM $CdCl_2$ + 0.2 mm $CaCl_2$ for up to 24 hours. Subcellular compartments were surgically isolated at the indicated times. Each point represents the mean and standard error of 3 or 4 individually exposed cells.

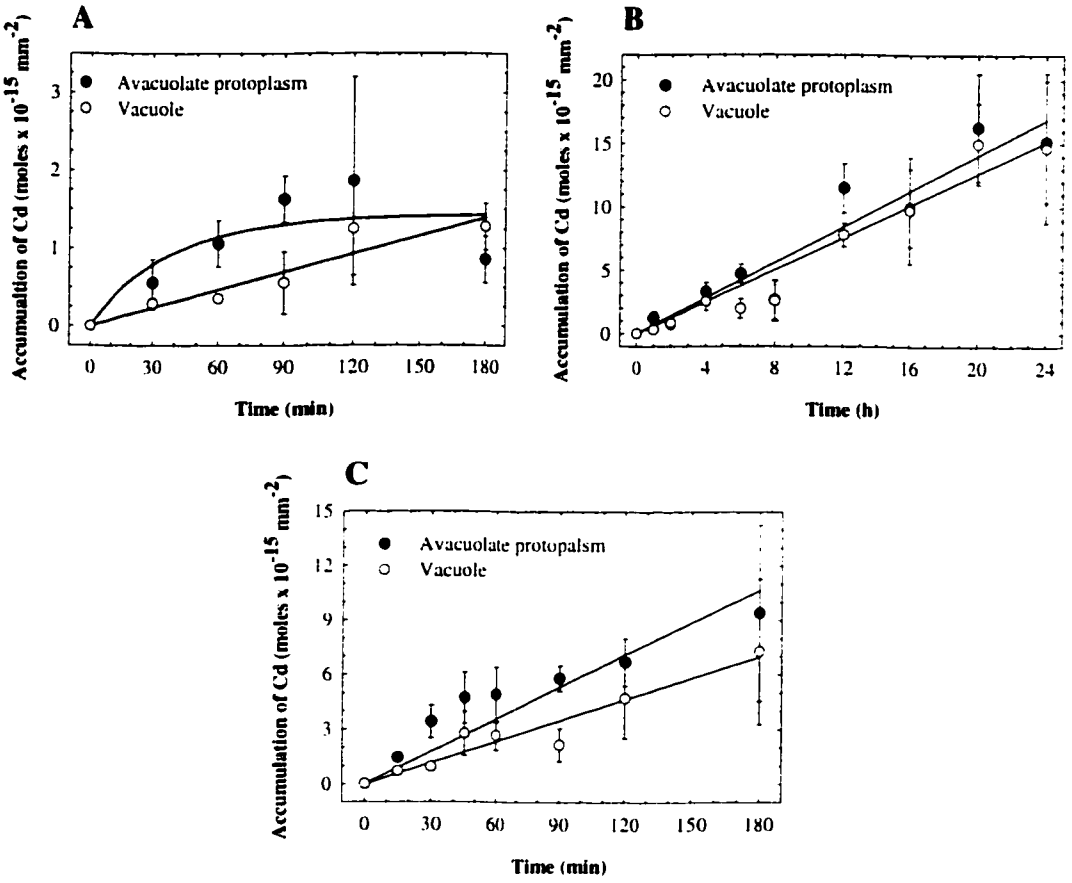

Figure 2.7. Protoplasmic accumulation and localization of cadmium. Individual internodal cells of *Chara corallina* were exposed to a radiolabeled solution of $CdCl_2$ + 0.2 mM $CaCl_2$. (**A**) 1 nM exposure over a 3 hour period. (**B**) 1 nM exposure over a 24 hour period. (**C**) 10 nM exposure over a 3 hour period. Each point represents the mean and standard error of 3 or 4 individually exposed cells.

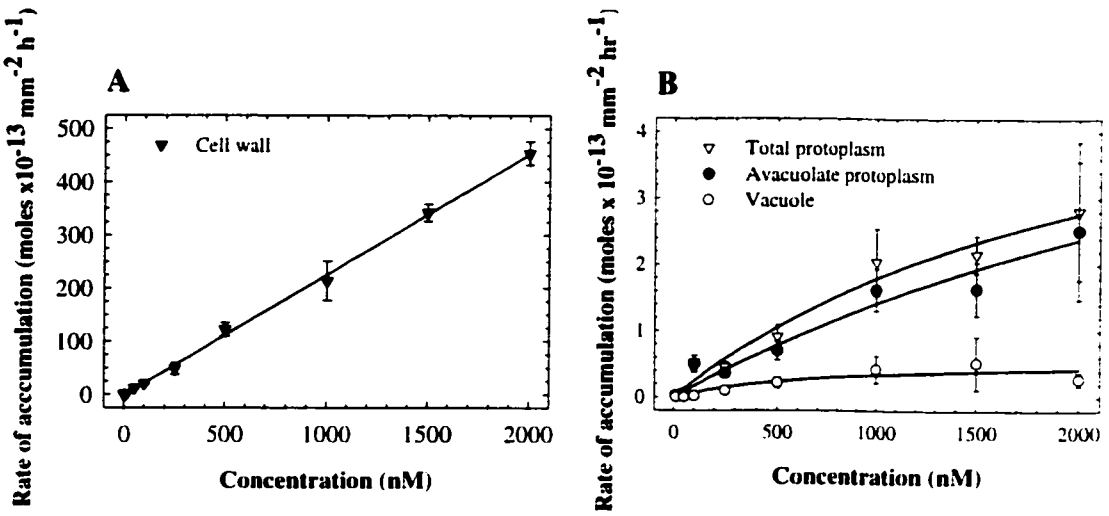

Figure 2.8. Kinetics of cadmium accumulation. Individual internodal cells of *Chara corallina* were exposed to a radiolabeled solution of $CdCl_2$ + 0.2 mM $CaCl_2$ for 30 minutes. Subcellular compartments were then surgically isolated. (**A**) Rate of Cd accumulation in the cell wall, (**B**) rate of Cd accumulation into the total protoplasm, avacuolate protoplasm, and the vacuole. Each data point represents the mean and standard error of 4 or 5 individually exposed cells.

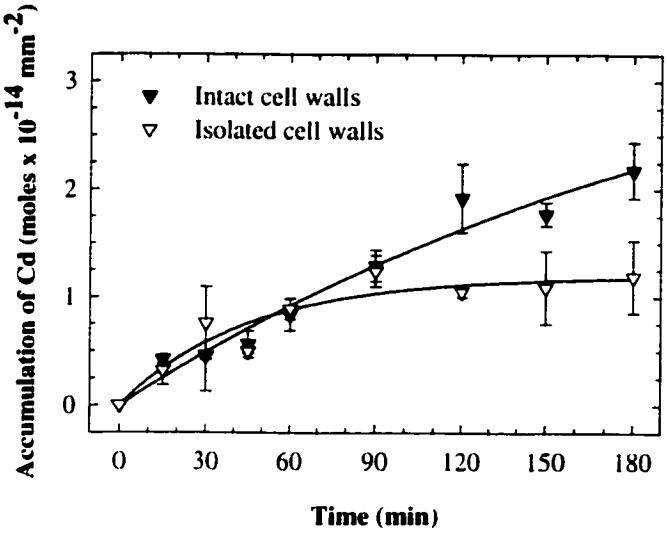

Figure 2.9. The time course of Cd accumulation in intact and pre-exposure isolated cell walls. Intact and pre-exposure isolated cell walls were exposed to 1 nM $CdCl_2$ + 0.2 mm $CaCl_2$ for up to 3 hours. Cell walls of intact cells were surgically isolated following exposure. Each point represents the mean and standard error of 3 or 4 individually exposed cells or cell walls.

Table 2.1. The rate of accumulation of cadmium in the cell wall and total protoplasm of internodal cells of *Chara corallina*. Accumulation rates were calculated from data in Fig. 2.5.

Concentration of uptake solution (nM)	Exposure time[a] (min)	Cell wall (moles x 10^{-14} mm^{-2} h^{-1})	Total protoplasm (moles x 10^{-15} mm^{-2} h^{-1})
1	0-30	2.00 ± 0.25	NA[b]
	45-180	0.62 ± 0.12	NA
	0-180	NA	1.54 ± 0.16
10	0-30	53.4 ± 0.6	NA
	45-180	5.6 ± 0.5	NA
	0-180	NA	5.16 ± 0.47
100	0-30	262 ± 40	NA
	45-180	72 ± 16	NA
	0-60	NA	99.6 ± 32.4[c]

[a] time of exposure over which the accumulation rate was calculated, [b] results not applicable to time frame, [c] saturation observed after 60-90 minutes.

Table 2.2. Kinetic constants for cadmium accumulation in internodal cells of *Chara corallina*. Values were determined by fitting data from Fig. 2.7 to the Michaelis-Menton equation ($y = (V_{max}*x)/(K_m+x)$) within Sigmaplot 2000 (SPSS), and calculating K_m and V_{max}. Values are presented with associated standard error. P-values for each value are listed in parentheses and were obtained from Sigmaplot 2000.

	V_{max} (moles x 10^{-13} mm^{-2} h^{-1})		K_m (moles x 10^{-9})	
Total protoplasm	6.07 ± 1.83	(0.02)	2400 ± 1100	(0.08)
Avacuolate protoplasm	7.58 ± 5.10	(0.21)	4400 ± 4000	(0.36)
Vacuole	0.58 ± 0.22	(0.04)	700 ± 700	(0.33)

Table 2.3. Subcellular accumulation of cadmium in internodal cells in the presence and absence of metabolic inhibitors, low temperature, or the protoplasm. Single internodal cells were exposed to 1 nM $CdCl_2$ + 0.2 mM $CaCl_2$ for 3 hours, in the presence or absence of the metabolism inhibiting treatment, then surgically separated into subcellular components. The pre-isolated cell walls were surgically separated prior to $CaCl_2$ pretreatment.

Treatment	Cadmium amount in fraction (moles x 10^{-14} mm^{-2})			
	Cell wall	Total protoplasm	Avacuolate protoplasm	Vacuole
$CdCl_2$ (control)	5.14 ± 1.0	0.22 ± 0.10	0.13 ± 0.07	0.09 ± 0.04
$CdCl_2$ + DNP	4.70 ± 0.5	0.10 ± 0.02	0.06 ± 0.01	0.04 ± 0.01
$CdCl_2$ + CCCP	4.65 ± 0.8	0.05 ± 0.01	0.04 ± 0.01	0.02 ± 0.01
$CdCl_2$ @ 4 °C	3.33 ± 0.3*	0.04 ± 0.01	0.03 ± 0.01	0.01 ± 0.01
Pre-isolated cell walls + $CdCl_2$	3.20 ± 0.3*	NA	NA	NA
Pre-isolated cell walls +$CdCl_2$ @ 4 °C	2.40 ± 0.2*	NA	NA	NA

NA— non applicable, DNP—2,4 dinitrophenol, CCCP— m-chloro carbonyl cyanide phenylhydrazine. * indicates a significant difference from the control ($p < 0.05$).

Chapter 3. The nature of cadmium accumulation in the cell wall of *Chara corallina*

3.1. Introduction

Experiments examining accumulation of cadmium (Cd) in internodal cells of *Chara corallina* (Chapter 2) indicated that the cell wall is the largest sink for accumulated Cd in this species. Estimates of Cd accumulation in cell walls of *Chara corallina* (>85% of total) and the apoplasm of plant roots (30-50% of total) vary considerably. Such variability could arise from inter-specific differences, different exposure solution compositions, or misinterpretation of experimental data.

Measurements of Cd levels in cell wall pools have frequently relied on desorption techniques, and two procedures have been traditionally used. The first procedure involves exposing roots to experimental solutions containing ^{109}Cd for accumulation, followed by desorption in an excess of unlabeled Cd. Cadmium desorbed from the tissue is then calculated based on the amount of isotope present in the desorption solution (Cataldo *et al.*1983), or the amount of Cd remaining in the tissue (Hart *et al.*1998). This method allows for a direct measure of exchangeable Cd from the root tissue over a specific time period. Profiles of Cd desorption (Cd desorption from root tissue over time) can be constructed by desorbing numerous root samples, each over a specific time period (0, 2, or 5, or 10, or 15 min, etc, Hart *et al.* 1998), and the amount of Cd remaining plotted against the desorption time. Using the desorption method, Cd bound to readily-exchangeable sites in the apoplasm of soybean (after a 1.5 hr desorption in 20-fold excess $CdCl_2$) has been shown to be concentration dependent and to range from 2 – 6% of total accumulation (Cataldo *et al.* 1983, Fig. 2.2A). In bread wheat this range was higher, approximately 8 – 30 % of total accumulated Cd, but Cd was desorbed for 1 hour in 117 – 1400 fold excess $CdSO_4$ (Hart *et al.* 1998). Both groups of authors observed that >90% of the readily-exchangeable Cd was removed after a 30 minute exposure to their respective desorption solutions.

A problem associated with this approach is the destructive nature of the sampling procedure. Cadmium levels in the root before and after desorption cannot be compared

in the same tissue sample. Differences in Cd accumulation between the two compared treatments (desorbed versus non-desorbed) could alter the amount of Cd perceived to be readily-exchangeable in the apoplastic pool. An additional drawback to this approach is that data for the profile would be collected from roots of numerous plants and would not take into account potential differences in total Cd accumulation between the different plants.

In contrast to measuring desorption from individual root samples at a single time point, some researchers have opted to use a second technique, the sequential desorption technique. With this approach, Cd desorbed from a single root sample is examined at all time points and used to construct a complete desorption profile. Sequential desorption of samples is conducted by transferring the tissue sample to fresh desorption solution at specific time points. The amount of radioactive ion desorbed over the time interval is then measured (see Table 3.1 for example), and a profile of Cd remaining in the tissue over time compiled. In contrast to the destructive sampling used in the single time point method above, the sequential desorption technique provides a direct comparison between Cd present before and after desorption of the root or cell. This is beneficial as a frame of reference is provided that can take into account differences in total accumulation by expressing the results as a percentage value rather than an absolute value. However, an implicit assumption associated with the technique is that the distribution of Cd (or cation) at exchangeable or non-exchangeable sites will be similar in any given plant, regardless of the absolute accumulation level. The sequential desorption technique was initially used to measure exchange properties and ion distribution of monovalent cations (K^+, Na^+) in single cells of *Nitellopsis obtusa* (MacRobbie and Dainty 1958), and root tissues of *Zea mays* L. (Kochain and Lucas 1982), *Pseudotsuga menziesii*, and *Hordeum vulgare* (Rygiewicz *et al.* 1984). Sequential desorption has since been used to the study the exchange of divalent cations. Desorption of Cd^{2+} has been reported from root tissue of *Agrostis gigantea*, and *Zea mays* L. (Rauser 1987), and from mycelia of the ectomycorrhizal fungus *Paxillus involutus* (Blaudez *et al.* 2000). Desorption of Zn^{2+} has been reported in root tissue of *Thlaspi caerulescens*, a Zn hyperaccumulator (Lasat *et al.* 1998).

The profile of desorption observed using sequential desorption has been interpreted to represent ions desorbed from numerous subcellular pools within a tissue or cell. These pools include the cell wall, cytoplasm, and vacuole (MacRobbie and Dainty 1958 – Fig. 3.1, Kochain and Lucas 1982, reviewed in Cheesman 1986, Lasat *et al.* 1998). Each pool is suggested to have a linear exchange function with respect to time, and the overall curve represents the addition of the multiple functions (Fig. 3.1). The linear functions were traditionally resolved by hand, but advances in non-linear regression analysis and computer-derived analysis have facilitated estimation of compartment sizes and exchange constants associated with the linear functions. Exchange times have been used to assign a specific pool to a subcellular location. The pool with the fastest exchange time has traditionally been assigned to the cell wall, and has been suggested to be Cd desorbed from readily-exchangeable sites. The pool with the second fastest exchange time has been traditionally assigned to the cytoplasm, and the slowest exchangeable pool has been assigned to the vacuole. It should be noted that the underlying assumption of this technique is that these subcellular pools act in series, and Cd movement between any two pools during desorption occurs at a single rate.

Using the sequential desorption technique, the amount of readily-exchangeable divalent cations present in the cell wall has been reported to be 50% of total Cd in the fungus *Paxillus involutus* (Blaudez *et al.* 2000), and 61% of total Zn in *Thlaspi caerulescens* (Lasat *et al.* 1998). Pool sizes in *Agrostis gigantea* and *Zea mays* were not reported (Rauser 1987). Estimates of cell wall pool size obtained from sequential desorption studies were larger than the 10-25% of total estimated from studies using the single time point desorption approach (Cataldo *et al.* 1983, Hart *et al.* 1998). The discrepancy between results observed with these techniques has not been addressed in the literature. Differences in exposure times would alter the absolute amounts of Cd present in all subcellular pools, and the resulting desorption profile would vary accordingly. It is also possible that the short desorption times employed when using the single time point method did not allow observation of the slower exchanging components. Regardless of the technique used, a direct measure of Cd desorbing from specific subcellular location was not achieved. Without this direct measure, the assignment of desorbed cation pools

to specific subcellular locations from data compiled by one or both or these experimental approaches is speculative at this time. Even with this problem, the sequential desorption technique has been given merit for determining wash (desorption) times for removal of readily-exchangeable Cd from the cell wall and the approximate size of the cell wall pool (Cheesman 1986).

The objective of research presented in this chapter was to determine the nature of Cd accumulation within the large, cell wall pool in internodal cells of *Chara corallina*. This was determined using the sequential desorption technique as the primary experimental approach. Results obtained can also be compared to single time point desorption experiments. *Chara corallina* is a powerful model system in that a direct comparison between the techniques is feasible due to surgical techniques that allow a direct measurement of the cell wall, avacuolate protoplasm and the vacuole following desorption. The amount of Cd present in readily-and non-exchangeable sites in internodal cell walls will be reported and compared to previous reports from root tissues. Direct measurement of desorption from the protoplasmic components will also be reported.

3.2. Materials and Methods

3.2.1. Exposure conditions

Internodal cells of *Chara corallina* were harvested and prepared for exposure as described in Chapter 2. After pretreatment, single viable cells were exposed for 3 hours to 110 ml of 1 nM $CdCl_2$ + 0.2 mM $CaCl_2$ labeled with ^{109}Cd as a tracer. Specific activity of ^{109}Cd ranged from 24–58 MBq μg^{-1}, but was constant for a given experiment. Following exposure, cells were briefly rinsed (2 sec) in 0.2 mM $CaCl_2$. In some treatments, cell walls were surgically isolated as described in Chapter 2, length and diameter were measured, and subjected to the desorption treatment. In other treatments, cell walls were isolated after desorption. Intact cells were briefly rinsed (2 sec) in 0.2 mM $CaCl_2$ following exposure to ^{109}Cd, and immediately desorbed as described below. Following desorption, cell walls were surgically isolated as described in Chapter 2. All solutions (both exposure and desorption) were equilibrated to pH 6.0 with KOH or HCl.

3.2.2. Desorption protocol – sequential desorption method

The desorption protocol used here was similar to that used previously for compartmental efflux analysis of cell wall and intracellular pools of ^{109}Cd from plant roots (Cheesman 1986, Rauser 1987) and fungi (Blaudez *et al.* 2000), and to that used for estimating desorption of ^{65}Zn pools from plant roots (Lasat *et al.* 1998). Sequential desorption of Cd from isolated cell walls or intact cells was carried out by transferring the cells or cell walls to fresh desorption solution at selected time points during desorption (see Table 3.1 for example). This resulted in the compilation of a full Cd desorption profile from each replicate. A group of 5 isolated cell walls or intact cells was considered an individual replicate, as ^{109}Cd desorbed during experiments with single intact cells fell under the detection limits. No differences were observed between desorption profiles compiled using either a single isolated cell wall or a group of 5 isolated cell walls as a single replicate. Results were expressed as the percentage of Cd remaining in the cell wall [((total desorption) – desorption$_{(t=x)}$)/(total desorption) *100%] at a given desorption time point. I reasoned that the percentage of total Cd desorbed from a given cell wall should be similar at a given time point regardless of the absolute amount of Cd being desorbed. This allowed data to be normalized for differences in absolute Cd accumulation between individual samples. Statistical analysis of data was conducted using the linear and non-linear regression functions within Sigmaplot 2000 (SPSS Inc).

3.2.3. The effect of desorption solution composition on cadmium desorption from isolated cell walls

Following exposure, groups of isolated cell walls were desorbed at 4 °C in 5 mL of an appropriate desorption solution within 50 ml plastic beakers. The solutions compared were 100 nM $CdCl_2$, 75 nM DTPA (diethylenetriamine pentaacetic acid, a cation chelator), 100 nM $CdCl_2$ + 0.2 mM $CaCl_2$, 75 nM DTPA + 0.2 mM $CaCl_2$, 0.2 mM $CdCl_2$, 0.2 mM $CaCl_2$, and 0.2 mM $CdCl_2$ + 0.2 mM $CaCl_2$ (the absolute amount of Cd or DTPA present in 5 mL of any desorption solution was sufficient to either exchange or chelate all Cd present in the group of cell walls after a 3 hour exposure to 1 nM $CdCl_2$). Beakers containing desorption solutions were continually stirred on a flatbed shaker. Measurements of Cd desorption were taken over 180-minute (1, 2, 5, 8, 10, 15, 30, 45,

60, 90, 120, and 180 min) and 12 hour (0.25, 0.5, 0.75, 1, 1.5, 2, 4, 6, 8, and 12 hr) time periods. Radioactive ^{109}Cd present in desorbed solutions was assayed by gamma counting of 3 mL samples, and expressed as a percentage of total ^{109}Cd remaining in the cell wall at a given time point. Each time point within a desorption profile represented the mean and standard error of 3 individual replicates.

3.2.4. Comparison of desorption profiles from intact and isolated cell walls

Individual internodal cells were exposed to ^{109}Cd labeled solutions (1 nM $CdCl_2$ + 0.2 mM $CaCl_2$, activity- 24–58 MBq μg^{-1}) for 3 hours. Following exposure to the experimental solution, intact cells were briefly rinsed (2 sec) in 0.2 mM $CaCl_2$ then pooled into groups of 5 (each group a single replicate) for desorption. A second series of replicates of isolated cell walls was prepared by surgical isolation following Cd exposure. Desorption of all replicates was conducted in 25 mL of 100 nM $CdCl_2$ + 0.2 mM $CaCl_2$ at 4 °C with ^{109}Cd measured from 3 mL samples of desorption solution at 1, 2, 5, 8, 10, 15, 20, 30, 45, 60, 90, 120, and 180 minute intervals. Low temperatures were used to reduce cellular metabolism and active accumulation of Cd in the protoplasm beyond the exposure period. Desorption of all samples was conducted in plastic petri dishes (11x150 mm, Fischer Scientific) to keep the intact cells submerged during the desorption treatment. This was necessary due to the length of the intact cells and the fact they are less flexible than the isolated cell walls. Desorption solutions were continually stirred as described above. Results were expressed as the percentage of ^{109}Cd remaining in cell walls. Each point within a desorption profile represented the mean and standard error of 3 individually desorbed replicates.

The amount of Cd remaining in the intracellular fractions of internodal cells after desorption was also directly determined. Internodal cells were each exposed to 110 mL of 1 nM $CdCl_2$ + 0.2 mM $CaCl_2$ radiolabeled with ^{109}Cd for 3 hours in the exposure chambers described in Chapter 2. Following exposure, all solution was removed and replaced with 100 nM $CdCl_2$ and 0.2 mM $CaCl_2$. The large volume of desorption solution used was required to completely cover the internodal cells within the exposure chambers. Cells were removed from desorption solution after 30 or 180 minutes and

subcellular fractions were surgically isolated. Radioactive Cd measured in each subcellular fraction was compared to the levels present in subcellular fractions from cells exposed to experimental solution for 3 hours, but not subjected to the desorption treatment. Each time point represents the mean and standard error of 4 individually exposed and desorbed cells.

Desorption profiles were also constructed from cell walls surgically isolated prior to ^{109}Cd exposure. Isolated cell walls were each exposed to 110 mL of 1 nM $CdCl_2$ + 0.2 mM $CaCl_2$ labeled with ^{109}Cd. Cell walls were grouped into replicates after exposure and each replicate was desorbed in 100 nM $CdCl_2$ + 0.2 mM $CaCl_2$. Desorbed ^{109}Cd was measured from 3 mL samples of desorption solution collected at 1, 2, 5, 8, 10, 15, 20, 30, 45, 60, 90, 120, and 180 minute intervals. Each data point within a profile represents the mean and standard error of 3 individually desorbed replicates. The percent of Cd remaining in the cell wall over time in these pre-isolated cell walls was compared to the desorption profiles of intact cells, and cell walls isolated following ^{109}Cd exposure.

3.3. Results and Discussion

3.3.1. Comparison of desorption treatments

Before the effect of solution composition on desorption could be examined, the desorption unit needed to be defined. When desorption profiles using an individual cell wall as a replicate were compared to profiles from groups of 5 cells walls per replicate (exposed to 5 mL of desorption solution), no difference in total desorption was observed (Fig. 3.2). However, analysis of desorption solutions from individual cell walls desorbed in 25 mL of solution failed to detect desorbed ^{109}Cd during the 1, 2, and 5 minute time points. Therefore, groups of 5 cell walls were used as individual replicates for subsequent desorption experiments.

Experiments were then conducted to determine which desorption solution was most effective at removing the readily-exchangeable pool of cell wall associated Cd. The desorption agents examined included excess unlabelled Cd and the cation chelator DTPA. Since DTPA had proved effective at removing and estimating extractable Cd from soil

samples (Bailey *et al.* 1995), it was hypothesized that it might effectively remove readily-exchangeable Cd from cell walls. Both desorption agents were able to remove the readily-exchangeable Cd component (Fig. 3.3A), and desorption appeared to continue through 3 hours. However, 100-fold excess Cd desorbed more ^{109}Cd than the DTPA treatment. When 0.2 mM $CaCl_2$ (background solution) was included in the desorption solution, the desorption efficiency of both agents increased, but the relative desorption capabilities remained similar (Fig 3.3B, excess Cd was a better agent). From this point on, a 100-fold excess $CdCl_2$ was used as the desorption agent.

Including 0.2 mM $CaCl_2$ in desorption solutions increased the concentration of competing cations in solution by 2000-fold. To test the effect of this increase in cations on desorption, $CdCl_2$ and $CaCl_2$ alone and in concert were examined as desorption agents at the increased concentration (0.2 mM; Fig. 3.4). High concentrations of $CdCl_2$, $CaCl_2$, or both together, were not as effective in removing the exchangeable component as 100 nM $CdCl_2$ + 0.2 mM $CaCl_2$. Desorption in this experiment was slower than previously observed. Differences may have been due to variation in the number of exchangeable cell wall sites between cultures grown in different tanks. Still, exchange appeared to be continuing though the longest desorption point (12 h). It was puzzling that the large excess of both Cd and Ca was not more effective at desorbing the radiolabel from the cell wall than the lower Cd concentration. Upon repeating the experiment identical results were obtained, giving me confidence this is an actual phenomenon. Nonetheless, I cannot yet explain the occurrence.

Results from these experiments were not fully comparable to previously published data as the desorption units were not identical. Studies conducted on root tissues and *Nitellopsis* cells used intact, initially viable tissue or cell samples for both exposure and desorption. In these experiments, viable internodal cells were exposed, but cell walls were isolated prior to desorption. To compare desorption profiles from cell walls of internodal cells of *Chara corallina* to profiles from cells of *Nitellopsis* or root tissues, desorption profiles from intact cells were compiled.

3.3.2. Desorption of intact versus isolated cell walls

Desorption of isolated cell walls eliminates any interplay between the protoplasm, cell wall, and extracellular spaces interpreted to occur from previous sequential desorption studies. When the desorption profiles of intact and isolated internodal cell walls were compared, a similar pattern of Cd desorption was observed (Fig. 3.5). Fitting non-linear regression functions to the data for both intact cell walls and isolated cell walls indicated that a two-component model for desorption provided the best fit for the data, suggesting two separate pools of exchangeable Cd (Table 3.2, 3.3). A one pool model also provided a good statistical fit (Table 3.2, 3.3), however, graphical interpretation and R^2 values associated with the one pool model gave a poorer representation of experimental data compared to other models examined (Table 3.2, Table 3.3, Fig. 3.6). The one pool model was then discarded. Two and three pool models were also fit to the intact and isolated cell wall data with and without addition of a fixed non-exchangeable component. Different research approaches have suggested both the presence (single time point desorption) and absence (sequential desorption) of a non-exchangeable cell wall component. Adding a fixed component to the mathematical equation (y^0) provides a means of modeling this non-exchangeable component. The R^2 values for 2 and 3 pool models with and without the fixed component suggested a good fit ($R^2 \sim 0.998$, Table 3.2, Table 3.3). However, estimation of pool sizes and exchange constants from models containing the fixed component had higher P-values associated with them than did the 2 pool model alone (Table 3.2, Table 3.3). The 2 component model was accepted to be the best representation of the data for both isolated and intact cell wall desorption profiles.

The two pools predicted to be present were designated as 'fast' or 'slow' based on the calculated half time for exchange. The 'fast' pool had a half time for exchange in the order of minutes. The 'slow' pool had a half time of exchange of hours (Table 3.2, 3.3). Both cell wall pools were present in intact and isolated cell walls and were similar in size. However, a difference between desorption of intact and isolated cell walls appears to be the rapid exchange of Cd in the fast pool. As the only difference between the desorbed samples is the absence of a functional protoplasm, an aspect of cellular metabolism not affected by the low temperature conditions, or the plasma membrane potential could

alter the desorption rate of the fast cell wall component. Desorption of Cd was also observed from the avacuolate protoplasm (Fig. 3.7), but not the vacuole over the three hour time desorption time. The total amount of Cd desorbed from the avacuolate protoplasm after 30 minutes could not account for the difference between intact and isolated cell walls over the same time frame.

Results reported here differ from those observed in single time point desorption analyses of root tissues. Tissue studies suggested rapid removal of the readily-exchanging component from the apoplasm (>90% of readily-exchangeable cell wall Cd removed in ~30 minutes; Cataldo *et al.* 1983, Hart *et al.* 1998). In contrast, desorption of Cd from cell walls of intact or isolated internodal cells continued through the last time point in all experiments conducted (3 or 12 hr). In previous studies, the readily-exchanging Cd component accounted for 2% of total accumulation in soybean roots (Fig. 2.2A, Cataldo *et al.* 1983), and 10% of the total in wheat roots (70 nM exposure, 1 hr desorption, Hart *et al.*1998). The remainder of the putative apoplasmic Cd fraction was suggested bound to non-exchangeable sites in the apoplasm. Results obtained with internodal cells of *Chara corallina* suggest that all Cd associated with the cell wall is exchangeable (Table 3.2, Table 3.3).

The percentage of desorbed Cd fluctuated between experiments. This variation could have been due to several possibilities. First, differences between the cultures (most probably age of internodal cells) could have resulted in different exchange properties. Fewer binding sites could have been present in one culture. Second, as long term desorption studies were conducted with isolated cell walls in smaller amounts of desorption solutions (5 mL), an equilibrium between ^{109}Cd in the cell walls and solution could have occurred during longer periods between solution changes. Reduced desorption from these treatments would have been observed. Also, the increase in the absolute amount of desorbing ions in 25 mL of solution compared to 5 mL could have resulted in an increased desorption rate when 25 mL of solution was used, even though the desorption solution concentration remained the same. It should be noted that

regardless of the method used (beakers versus Petri dishes), all accumulated Cd was suggested to be desorbable and the two pool model provided the best fit.

A comparison of desorption profiles from internodal cells of *Chara corallina* to those from previous sequential desorption analyses yielded some similarities. Studies with the ectomycorrhizal fungus *Paxillus involutus* (Blaudez *et al.* 2000) suggested a large readily-exchangeable component within the cell wall (50% of desorbed Cd). Also, Blaudez *et al.* (2000) suggested that all accumulated Cd was desorbable over time. This hypothesis was not tested due to the time necessary to desorb all Cd from the vacuole component ($t_{1/2}$ for exchange at hundreds of minutes). Desorption of Zn from the hyperaccumulator, *Thlaspi caerulescens*, also suggested a large rapidly-exchanging cell wall pool, accounting for 61% of total desorbed Zn (Lasat *et al.* 1998). It should be noted that the amount of non-exchangeable Zn potentially present in the cell wall was not reported. To date, the presence of a non-exchangeable pool in the cell wall has not been suggested or extrapolated from sequential desorption profiles. Full tissue desorption (over the vacuolar exchange period) would be required to investigate the presence of this component. To my knowledge, experiments conducted over this time frame have not been reported. Desorption of Cd from internodal cells of *Chara corallina* showed no indication of halting. Examination of multiple non-linear regression functions suggested that all Cd present in internodal cell walls was exchangeable. If the regression model was designed to include a fixed component (y^0 - non-exchangeable Cd), the resulting pool sizes or exchange constants had higher associated standard error and provided a poorer statistical fit (Table 3.2, Table 3.3). This held true for both the intact cell and the isolated cell wall desorption profiles.

The non-linear regression analysis suggested that two pools are present in intact and isolated internodal cell walls. Each pool is of a similar size in both cell wall treatments (Table 3.2, Table 3.3). This suggests the presence of multiple exchange sites within the cell wall. The most obvious difference between these pools is the smaller half time for exchange associated with the 'fast' exchanging pool from intact cell walls (4 min) compared to its counterpart in the isolated cell walls (14 min; Table 3.2, Table

3.3). As the exchange rate from this pool alone differs when the protoplasm is removed, cellular metabolism or membrane potential may play a role in regulating desorption of Cd from these 'fast' sites. Additional evidence for this interpretation was supplied by experiments where cell walls from internodal cells were isolated before exposure (pre-isolated group, Fig. 3.8), exposed to Cd, and then desorbed. The same desorption pools were observed in the pre-exposure isolated cell walls as in both the intact and isolated cell walls discussed above. As well, the exchange properties of the pre-isolated cell walls mirror those of isolated cell walls (Table 3.4). The faster 1/2 times for exchange of Cd pools in the pre-exposure isolated cell wall group were not unexpected. This can be explained by the fact that pre-exposure isolated cell walls accumulated less Cd that the intact or isolated cell wall groups. If the ratio of the amount of desorbing Cd ions to accumulated Cd influences the rate of desorption (as suggested previously), then the increased ratio found during desorption of the pre-exposure isolated group would allow for quicker desorption.

One explanation for the differences observed between this study and previous sequential desorption experiments is that the compartmental efflux interpretation may not be appropriate for studies conducted with divalent cations. When sequential desorption was first used on single cells of *Nitellopsis obtusa* to study desorption of monovalent cations (MacRobbie and Dainty 1958), subcellular fractionation techniques, similar to those used in this study, were employed to obtain an independent assessment of the cations remaining at various times during desorption. When these directly assessed values were compared to those observed during sequential desorption, they were approximately equal. The authors were then able to ascertain the specific subcellular location of the desorbed ions by examining the rate of desorption from the sequential analysis and the direct measurement methods. As a note, most of the radiolabel was associated with the protoplasm in the work of MacRobbie and Dainty (1958). When Kochain and Lucas (1982) examined K^+ influx and efflux in corn roots (an adaptation of the same technique) using $^{86}Rb^+$ as an analogue, most accumulated Rb^+ was also suggested to be symplasmic. Furthermore, when isolated cell wall preparations were exposed to $^{86}Rb^+$, little accumulation of radiolabel was observed. Interpretation of the

desorption profile was also based on the suggested symplastic nature of cation accumulation, but without a direct assessment of cation location to corroborate the interpretation. When utilizing the compartmental efflux interpretation with divalent cations, differences in the pattern of accumulation between monovalent and divalent cations may not have been considered. In studies examining divalent cation accumulation, a large component (30-50%) has been interpreted as cell wall accumulation. Due to the complex chemistry of constituents that comprise the cell wall, it may not be reasonable to assume a single rate of exchange between divalent cations in the cell wall and solution. More importantly, a direct assessment of divalent cation desorption from specific subcellular locations (similar to MacRobbie and Dainty 1958) has not been conducted to support assignment of pools calculated from sequential desorption profiles to specific locations. When Cd pools calculated from desorption profiles of internodal cells were compared to Cd pools remaining in specific locations after direct measurements (Fig. 3.5 and Fig. 3.7), the compartmental efflux interpretation could not explain the profiles.

Even though the compartmental efflux interpretation did not explain Cd desorption profiles from internodal cells, my results need not be mutually exclusive with those from previous desorption studies. It should be noted that I could have observed a pattern of desorption specific to Characean or other algal families. However, an alternate to the compartmental efflux interpretation can be hypothesized which takes into account an increased role for the plant cell wall in divalent cation accumulation and desorption. This alternate interpretation remains consistent with results from previous studies. In single time point desorption studies, short exposure times were employed (20 minutes, Hart *et al.* 1998). Shortened exposure periods would reduce the total amount of Cd accumulated by the tissue, but distribution between the cell wall pools should remain the same. If a cell wall pool, similar to the 'slow' exchanging pool identified here is also present in root tissues, exchange would not be readily observed over the short time period of desorption (30-60 minutes). Exchange of a 'fast' pool would be observed over this time and would depend on the size of the pool. With the sequential desorption experiments, the Cd pools could have originated from the cell wall as opposed to the

symplasm. Depending on exposure periods, Cd could move through the apoplastic pathway (cell wall and cell wall spaces) to the cortex of root tissue. The profile of desorption for Cd from root tissue would then represent a combination of the following:

a) exchange from multiple sites within a cell wall,
b) exchange from various cell layers within the root cortex, and
c) exchange from the symplasm.

As suggested by results from internodal cells (Fig. 3.7), desorption from the symplasm of root cells should still be occurring, but could be masked within the variation of a desorbing cell wall pool. The fact that the root is a complex tissue hampers complete and unequivocal assignment of calculated Cd pools to specific subcellular locations. It is important to note that until direct measurements of subcellular Cd can be made in vascular plant systems, this hypothesis will be difficult to address.

3.4. Conclusions

Employing the sequential desorption method, all Cd present in the cell wall appeared desorbable with 100-fold excess $CdCl_2$. Desorption of Cd followed a biphasic pattern and continued through the longest time points examined (3 or 12 h). The large amount of Cd desorption from cell walls suggested that the non-exchangeable Cd observed in previous single time point desorption studies is small or absent in internodal cells. Previous sequential desorption studies also suggest the absence of the non-exchangeable component (Blaudez *et al.* 2000, not modeled by Lasat *et al.* 1998). When single time point analysis was employed on internodal cells, Cd desorption continued through 3 hours, further indicating complete exchange of accumulated Cd. This discrepancy in the literature has not been investigated, but may represent differences in desorption procedures used.

Desorbed Cd pools originated in the cell wall as suggested by similar pool sizes within both intact and isolated cell walls. Cadmium desorption from the protoplasm of intact cells could not account for the differences observed between intact and isolated cell walls over the first 30 minutes of desorption. The potential for multiple binding sites

within the cell wall provides an alternate interpretation for previously compiled desorption profiles. This may reflect an incorrect usage of the compartmental efflux model when examining divalent cation desorption. Compartmental efflux was first used to describe monovalent cation efflux and localization in giant algae cells where direct confirmation of cation position could be ascertained. Desorption of divalent cations was assumed to occur by the same model, even though accumulation patterns were different and no direct examination of cation location was conducted. It may not be valid to assume that efflux of divalent cations would follow the same pattern as monovalent cations. The large component of Cd present in cell walls of internodal cells with multiple exchange constants introduces an alternate interpretation for sequential desorption profiles. It may be necessary to re-evaluate current desorption conclusions based on results form this study. Until a direct measurement of divalent cation location can be made in a single plant cell, full interpretation of desorption profiles will be incomplete.

3.5. References

Bailey, V.L., Grant, C.A., Racz, G.J., Bailey, L.D. 1995. A practical method for assessing cadmium levels in soil using the DTPA extraction technique with graphite furnace analysis. Commun. Soil Sci. Plant Anal. 26: 961-968.

Blaudez, D., Botton, B., Chalot, M. 2000. Cadmium uptake and subcellular compartmentation in the ectomycorrhizal fungus *Paxillus involutus*. Microbiology. 146: 1109-1117.

Cataldo, D.A., Garland, T.R., Wildung, R.E. 1983. Cadmium uptake kinetics in intact soybean plants. Plant Physiol. 73: 844-848.

Cheesman, J.M. 1986. Compartmental efflux analysis: an evaluation of the technique and its limitations. Plant Physiol. 80: 1006-1011.

Hart, J.J., Welch, R.M., Norvell, W.A., Sullivan, L.A., Kochain, L.V. 1998. Characterization of cadmium binding, uptake, and translocation in intact seedlings of bread and durum wheat cultivars. Plant Physiol. 116: 1413-1420.

Kochain, L.V., Lucas, W.J. 1982. Potassium transport in corn roots. I. Resolution of kinetics into a saturable and linear component. Plant Physiol. 70: 1723-1731.

Lasat, M.M., Baker, A.J.M., Kochain, L.V. 1998. Altered Zn compartmentation in the root symplasm and stimulated Zn absorption into the leaf as mechanisms involved in Zn hyperaccumulation in *Thlaspi caerulescens*. Plant Physiol. 118: 875-883.

MacRobbie, E.A.C., Dainty, J. 1958. Ion transport in *Nitellopsis obtusa*. J. Gen. Physiol. 42: 335-353.

Rauser, W.E. 1987. Compartmental efflux analysis and removal of extracellular cadmium from roots. Plant Physiol. 85: 62-65.

Rygiewicz, P.T., Bledsoe, C.S., Glass, A.D.M. 1984. A comparison of methods for determining compartmental analysis parameters. Plant Physiol. 76: 913-917.

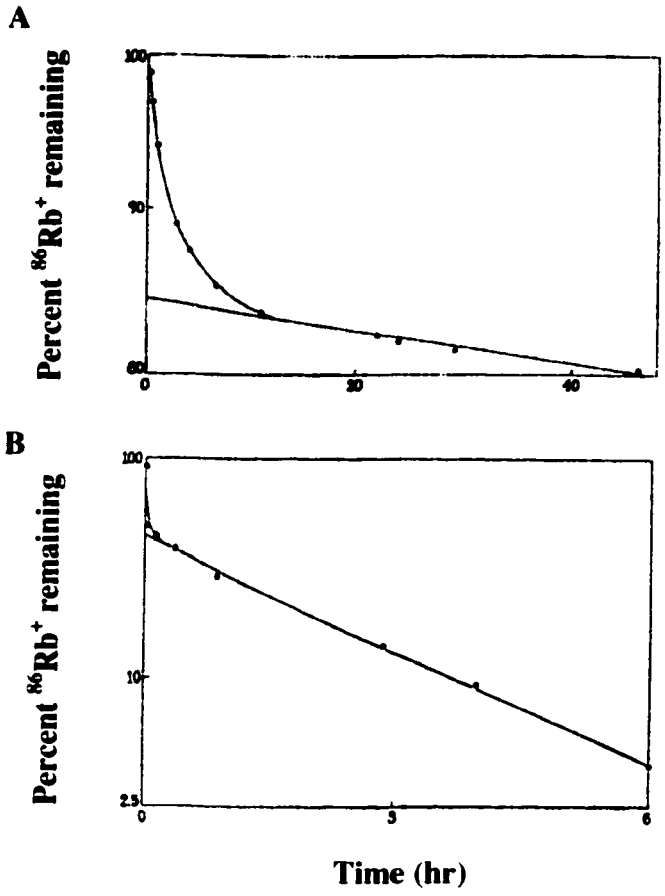

Figure 3.1. Sequential desorption of rubidium from single cells of the giant algae *Nitellopsis obtusa*, and the associated curve peeling technique for pool size estimation. (**A**) Full desorption profile with the linear component thought to represent Rb^+ present in the vacuole. The vacuolar component is then subtracted from the data, and the profile replotted (**B**). The next linear component is thought to represent Rb^+ present in the protoplasm. From MacRobbie and Dainty (1958).

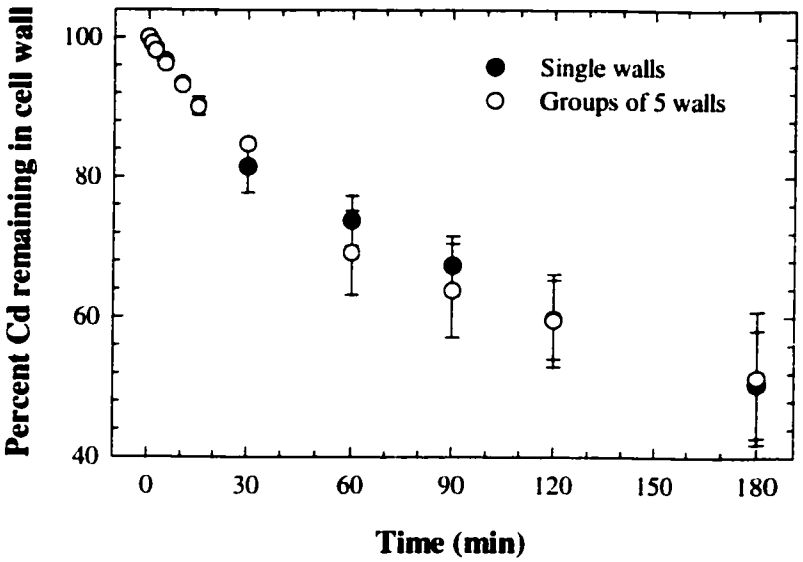

Figure 3.2. Comparison of Cd desorption from different desorption units. Desorption of individual cell walls or groups of 5 cell walls were compared as replicates. Internodal cells were exposed to 1 nM $CdCl_2$ + 0.2 mm $CaCl_2$ labeled with ^{109}Cd for 180 minutes. Cell walls were surgically isolated, placed into group of 5 or single cell wall replicates, then desorbed in 5 mL of 100 nM $CdCl_2$ + 0.2 mM $CaCl_2$ for 180 minutes. Data represent the mean and standard error of 3 individually desorbed replicates.

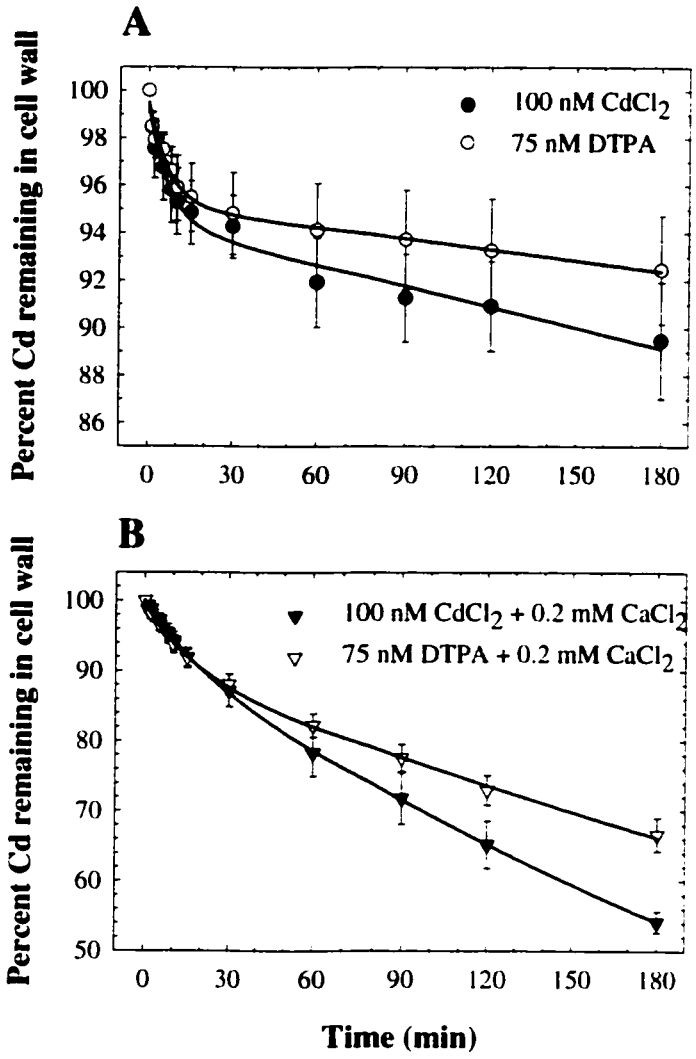

Figure 3.3. The effect of solution composition on desorption of Cd from internodal cell walls. Intact cells were exposed to 1 nM $CdCl_2$ + 0.2 mM $CaCl_2$ labeled with ^{109}Cd for 180 minutes and then cell walls were surgically isolated. Replicates (5 cell walls per replicate) were desorbed in 100 nM $CdCl_2$ or 75 nM DTPA with (**A**) or without (**B**) 0.2 mM $CaCl_2$. Data represent the mean and standard error of 3 individually desorbed replicates.

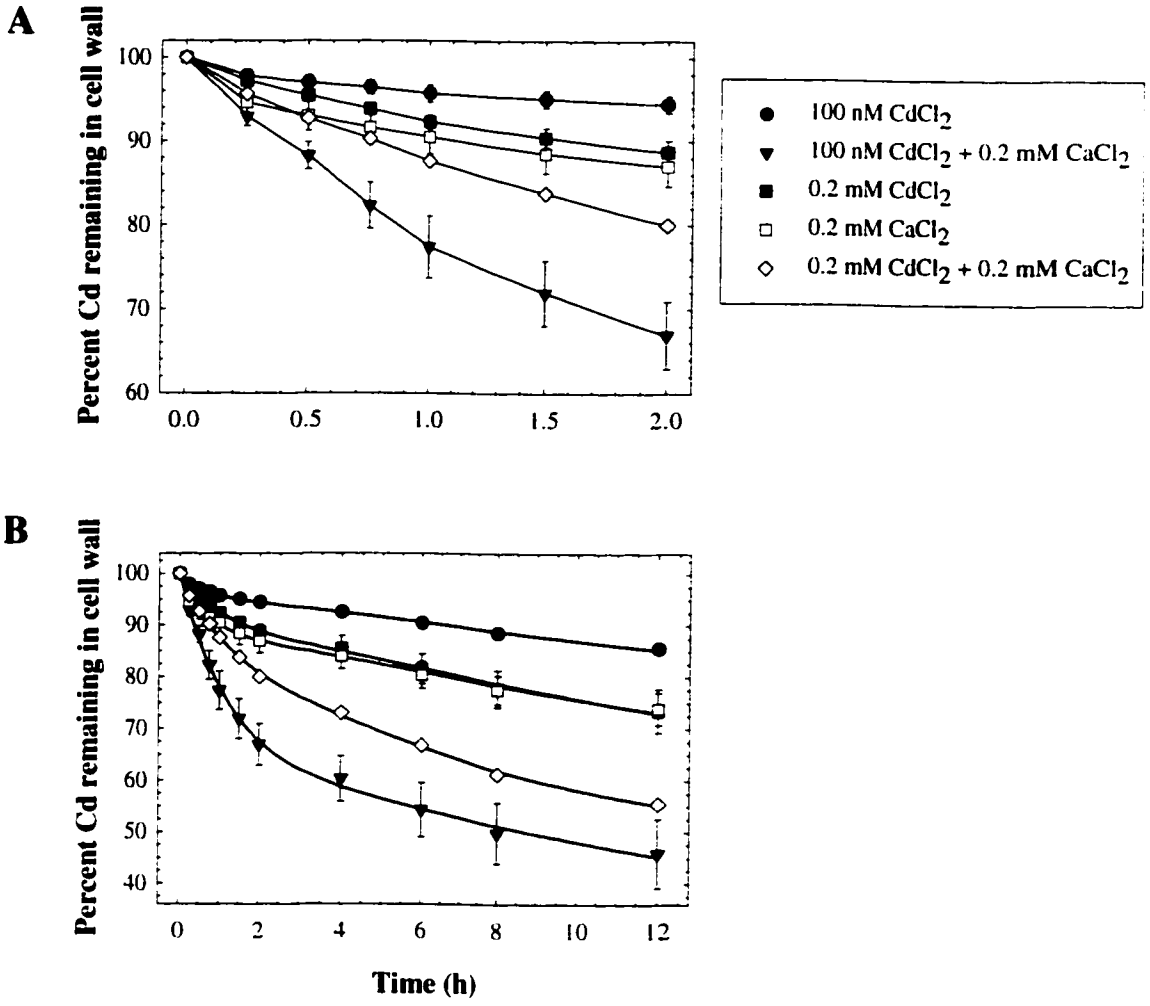

Figure 3.4. The effect of increased cation concentration on desorption of Cd from internodal cell walls. Internodal cells were exposed to 1 nM $CdCl_2$ + 0.2 mM $CaCl_2$ labeled with ^{109}Cd for 3 hours, then cell walls were surgically isolated. Replicates (5 cell walls per replicate) were desorbed for 12 hours in various concentrations of $CdCl_2$, $CaCl_2$, or both together. **(A)** Desorption of replicates over the first 2 hours, **(B)** full desorption profile over 12 hours. Data represent the mean and standard error of 3 individually desorbed replicates.

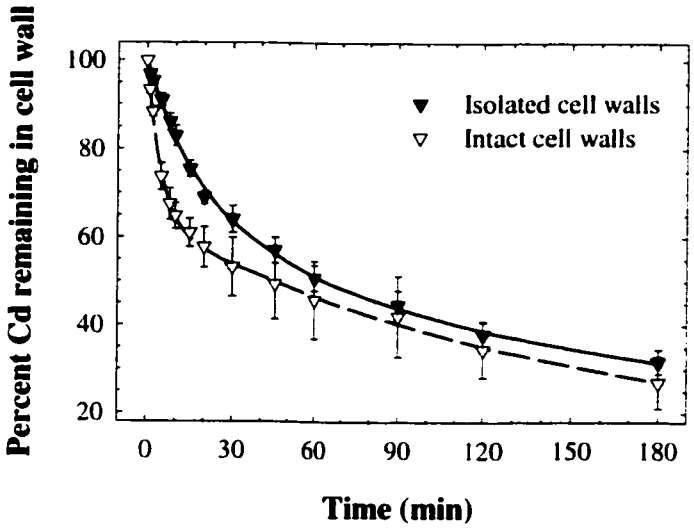

Figure 3.5. Desorption profiles from intact and isolated cell walls. Cells were exposed to 1 nM $CdCl_2$ + 0.2 mM $CaCl_2$ labeled with ^{109}Cd for 180 minutes. Replicates (groups of 5 cells or cell walls per replicate) were desorbed in 100 nM $CdCl_2$ + 0.2 mM $CaCl_2$ for a further 180 minutes. Intact cell walls (or cell walls of intact cells) were desorbed immediately following exposure, then surgically isolated. Isolated cell walls were collected following exposure, then desorbed. The function plotted for both data sets is a 2 parameter exponential decay model, as calculated by Sigmaplot 2000 (SPSS Inc.). Data represent the mean and standard error of 3 individually desorbed replicates.

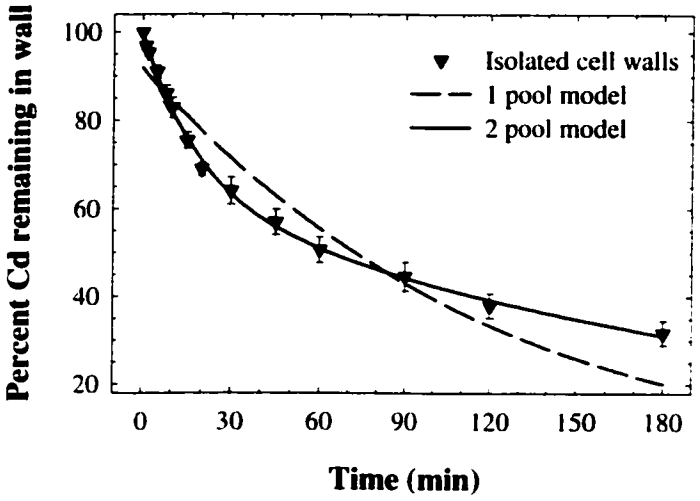

Figure 3.6. Non-linear regression analysis of the isolated cell wall desorption profile from Fig. 3.5. Desorption data from isolated cell walls was subjected to multiple non-linear regression analysis, and the resulting functions plotted (Table 3.2). The 2-pool model provided the best fit both graphically and statistically. Statistical models were calculated by Sigmaplot 2000 (SPSS Inc.).

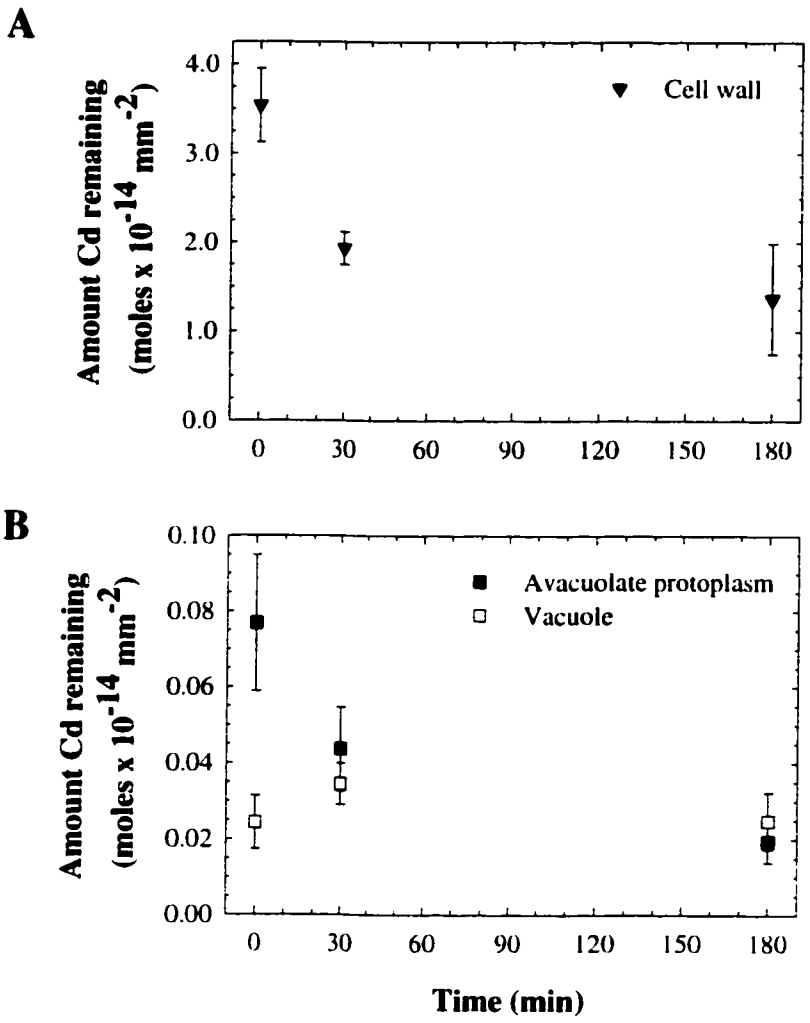

Figure 3.7. The amount of Cd remaining in subcellular compartments following desorption. Cells were exposed to 1 nM $CdCl_2$ + 0.2 mM $CaCl_2$ in 3-compartment chambers (see Chapter 1). Cells were desorbed (in the exposure chambers) in 100 nM $CdCl_2$ + 0.2 mM $CaCl_2$ for 0, 30, or 180 minutes and then surgically separated into subcellular components. **(A)** Amount of Cd remaining in cell wall. **(B)** Amount of Cd remaining in the avacuolate protoplasm and the vacuole. Data represent mean and standard of 5 individually exposed and desorbed cells.

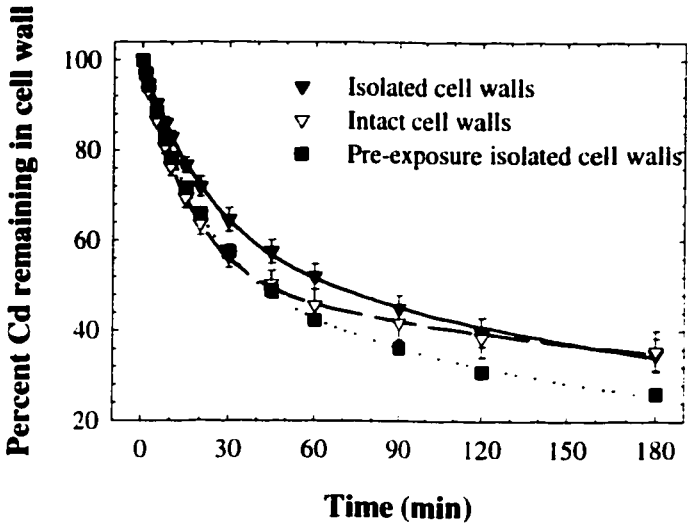

Figure 3.8. Cell wall desorption profiles of intact cells, isolated cell walls, and cell walls isolated prior to initial exposure (pre-isolated cell walls). The pre-isolated cell wall replicates were collected prior to Cd exposure. Intact and isolated cell wall replicates were collected after exposure as previously described. All replicates were exposed to 1 nM $CdCl_2$ + 0.2 mM $CaCl_2$ labeled with ^{109}Cd for 180 minutes. Replicates were then desorbed in 100 nM $CdCl_2$ + 0.2 mM $CaCl_2$ for a further 180 minutes and the percentage of ^{109}Cd remaining in the cell wall calculated. The function plotted for each data group is a 2 parameter exponential decay calculated by Sigmaplot 2000 (SPSS Inc.). Data represent the mean and standard error of 3 individually desorbed replicates.

Table 3.1. Sample sequential desorption time sequence. The amount of Cd desorbed at a given time point was calculated by summing Cd collected from all prior time points. (eg. 5 min total = $\sum$ (1 – 5 min points))

Total time point (min)	1	2	5	8	10	15	30
Time (min) exposed to fresh desorption solution	1	1	3	3	2	5	15

Table 3.2. Non-linear regression analysis parameters from multiple interpretations of the isolated cell wall data in Fig. 3.5. The 1-parameter curve was fit to $y = Ae^{(-Bx)}$, or $y = y^0 + Ae^{(-Bx)}$. The 2-parameter curve was fit to $y = Ae^{(-Bx)} + Ce^{(-Dx)}$, or $y = y^0 + Ae^{(-Bx)} + Ce^{(-Dx)}$. The 3-parameter curve was fit to $y = Ae^{(-Bx)} + Ce^{(-Dx)} + Ge^{(-Hx)}$, or $y = y^0 + Ae^{(-Bx)} + Ce^{(-Dx)} + Ge^{(-Hx)}$. The parameters A, C, and G represent cadmium present in different exchangeable pools. The parameters B, D, and H represent the exchange constants for exchange of cadmium from the respective pools. y^0 represents the y-axis intercept of an asymptote associated with the function. Values are reported with the associated standard error. The ½ time for exchange was calculated using the formula (0.693/exchange constant) as per Cheesman (1986). All analyses were conducted by the regression functions within the program Sigmaplot (v. 6.0, SPSS inc.). * indicates the best fit from both statistical and graphical analysis.

Regression analysis parameters	Pool	Size (% of total)	P-value	Exchange constant	P-value	½ time for exchange (min)	R^2 value
1	A	92 ± 2.6	<0.01	0.008 ± 0.001	<0.01	83	0.962
2*	A	38 ± 2.6	<0.01	0.051 ± 0.005	<0.01	14	0.998
	C	62 ± 2.7	<0.01	0.004 ± 0.001	<0.01	168	
3	A	31 ± 38	0.44	0.060 ± 0.042	0.19	11	0.998
	C	49 ± 490	0.92	0.008 ± 0.074	0.92	81	
	G	20 ± 530	0.97	0.000 ± 0.071	1.00	NC[a]	
1 + intercept	A	63 ± 1.9	<0.01	0.025 ± 0.002	<0.01	25	0.991
	y^0	35 ± 2.0	<0.01				
2 + intercept	A	31 ± 8.7	0.10	0.060 ± 0.012	<0.01	11	0.998
	C	49 ± 4.6	<0.01	0.008 ± 0.005	0.12	81	
	y^0	20 ± 11	0.10				
3 + intercept	A	31 ± 50	0.55	0.060 ± 0.051	0.28	11	0.998
	C	24 ± 2 x 10^7	1.00	0.008 ± 27.41	0.99	81	
	G	25 ± 2 x 10^7	1.00	0.008 ± 26.53	0.99	81	
	y^0	20 ± 180	0.92				

[a]NC – not calculable

Table 3.3. Non-linear regression analysis parameters from multiple interpretations of the intact cell wall data in Fig. 3.5. The 1-parameter curve was fit to $y = Ae^{(-Bx)}$, or $y = y^0 + Ae^{(-Bx)}$. The 2-parameter curve was fit to $y = Ae^{(-Bx)} + Ce^{(-Dx)}$, or $y = y^0 + Ae^{(-Bx)} + Ce^{(-Dx)}$. The 3-parameter curve was fit to $y = Ae^{(-Bx)} + Ce^{(-Dx)} + Ge^{(-Hx)}$, or $y = y^0 + Ae^{(-Bx)} + Ce^{(-Dx)} + Ge^{(-Hx)}$. The parameters A, C, and G represent cadmium present in different exchangeable pools. The parameters B, D, and H represent the exchange constants for exchange of cadmium from the respective pools. y^0 represents the y-axis intercept of an asymptote associated with the function. Values are reported with the associated standard error. The ½ time for exchange was calculated using the formula (0.693/exchange constant) as per Cheesman (1986). All analyses were conducted by the regression functions within the program Sigmaplot (v. 6.0, SPSS inc.). * indicates the best fit from both statistical and graphical analysis.

Regression analysis parameters	Pool	Size (% of total)	P-value	Exchange constant	P-value	½ time for exchange (min)	R^2 value
1	A	81 ± 4.2	<0.01	0.009 ± 0.002	<0.01	80	0.795
2*	A	39 ± 1.0	<0.01	0.192 ± 0.013	<0.01	4	0.998
	C	62 ± 0.9	<0.01	0.005 ± 0.002	<0.01	147	
3	A	32 ± 19	0.13	0.233 ± 0.098	0.03	3	0.998
	C	8.7 ± 17	0.63	0.072 ± 0.129	0.59	10	
	G	60 ± 2.9	<0.01	0.004 ± 0.001	<0.01	158	
1 + intercept	A	56 ± 4.3	<0.01	0.061 ± 0.013	<0.01	11	0.935
	y^0	39 ± 3.1	<0.01				
2 + intercept	A	38 ± 1.5	<0.01	0.199 ± 0.018	<0.01	4	0.998
	C	54 ± 8.4	<0.01	0.006 ± 0.002	<0.01	119	
	y^0	8.1 ± 9.5	0.42				
3 + intercept	A	32 ± 17	0.10	0.234 ± 0.086	0.03	3	0.998
	C	78 ± 130	0.57	0.003 ± 0.008	0.72	248	
	G	10 ± 10	0.32	0.060 ± 0.146	0.71	16	
	y^0	-10 ± 144	0.89				

Table 3.4. Non-linear regression analysis parameters from desorption of isolated, intact and pre-exposure isolated cell walls. Data from Fig. 3.8 was fit to the 2-parameter curve $y = Ae^{(-Bx)} + Ce^{(-Dx)}$. Values are reported with the associated standard error. The ½ time for exchange was calculated using the formula (0.693/exchange constant) as per Cheesman (1986). All analyses were conducted using the program Sigmaplot (v. 6.0, SPSS inc.).

Treatment	Pool	Size (% of total)	P-value	Exchange constant	P-value	½ time for exchange (min)
Intact cell walls	A	49 ± 1	<0.01	0.057 ± 0.002	<0.01	12
	B	50 ± 1	<0.01	0.002 ± 0.002	<0.01	347
Isolated cell walls	A	42 ± 2	<0.01	0.042 ± 0.003	<0.01	17
	B	57 ± 2	<0.01	0.003 ± 0.001	<0.01	230
Pre-exposure isolated cell walls	A	50 ± 2	<0.01	0.046 ± 0.002	<0.01	15
	B	49 ± 2	<0.01	0.004 ± 0.001	<0.01	200

Chapter 4. Conclusions

4.1. General conclusions

Current assessments of Cd localization have been based on two types of indirect analytical approaches, alterations in cellular metabolism and sequential desorption analysis. Conclusions based on these approaches are different with no clear reasoning addressed in the literature. Cadmium accumulation in response to altered cellular metabolism (eg. Cataldo *et al.* 1983, Hart *et al.* 1998) suggested that the majority of Cd was accumulated in a metabolism-dependent manner (50-70%) and was localized to the symplasm. Data arising from sequential desorption of tissue segments (eg. Rauser 1987) or fungal mycelia (Blaudez *et al.* 2000) suggested that the majority of Cd was localized to the apoplasm (50-60%), an idea also supported by work with Zn (Lasat *et al.* 1998). Neither of these methods employed a direct measurement of Cd in either the apoplasm or the symplasm, therefore the pools of Cd collected could not be conclusively assigned to a specific subcellular location.

To provide a direct measurement of subcellular Cd location, I chose to use the giant freshwater algae *Chara corallina* as a model system. *Chara corallina* is an organism suited for direct measurements of Cd location. Single internodal cells from a plantlet can be surgically separated into subcellular components (cell wall, avacuolate protoplasm, and vacuole). This system is similar to that initially used to directly measure localization of monovalent cations by MacRobbie and Dainty (1958), Zn^{2+} influx by Reid *et al.* (1996), and accumulation of Al^{3+} by Taylor *et al.* (2000). Using ^{109}Cd, I exposed single internodal cells to Cd and measured Cd accumulation and rates of movement into each of the subcellular compartments. The results observed differed from those collected using both previous approaches.

Cadmium accumulation was found to be concentration dependent, agreeing with previous reports in the literature. The rate of Cd accumulation into the cell wall increased linearly up to 2000 nM $CdCl_2$. This result agreed with Hart *et al.*'s conclusion (1998) that the linear component of their observed biphasic accumulation curve was apoplasmic

in nature. However, in internodal cells of *Chara corallina*, the cell wall was the dominant point for Cd accumulation, comprising 85% of total Cd at 1 nM exposure. This value rose to 99.4% of total accumulation at 2000 nM exposure. These results differ by 30–50 % from total Cd accumulation suggested to be in the apoplasm in both soybean (Cataldo *et al.* 1983) and wheat (Hart *et al.* 1998). In both the wheat and soybean systems, the symplasm was thought to be the dominant point of Cd localization. My data are more consistent with estimations of apoplasmic Cd from sequential desorption studies. Blaudez *et al.* (2000) suggested that 33-48% of accumulated Cd was localized to the cell wall (depending on exposure time), and estimations of cell wall Zn by Lasat *et al.* (1998) were approximately 60% of total. The association of greater than 85% of accumulated Cd in *Chara corallina* cells is much closer to these values, but still shows differences.

These discrepancies can perhaps be explained by differences in the various techniques used to measure Cd pools and in the nature of assumptions used to assign the pools to the apoplasm. In studies conducted by Cataldo *et al.* (1983) and Hart *et al.* (1998), one assumption was that all Cd accumulating in a metabolism-dependent manner was localized to the symplasm. In my experiments, accumulation of Cd in the cell wall of *Chara corallina* internodal cells appeared to be partially dependent on the presence of a functional protoplasm. When metabolism was inhibited by cold temperature treatment, cell wall Cd accumulation was reduced by 33%. Cadmium accumulation in cell walls isolated prior to Cd exposure was also similar to results observed under cold temperature treatment. However, accumulation of Cd in the cell wall was not reduced upon exposure to the metabolic inhibitors DNP or CCCP. Identical results (with the exception of isolated cell walls, which were not examined) were reported during accumulation of Al^{3+} in *Chara corallina* internodal cells (Taylor *et al.* 2000). Results from this study suggest that some aspect of cellular metabolism, which is not affected by the metabolic inhibitors used, may serve as the driving force behind this extracellular accumulation. The low temperature treatment would have induced a widespread inhibition of cellular metabolic functions, reducing the role that the protoplasm (metabolism) would play in accumulation of Cd in the cell wall. This would explain the similarities between accumulation of Cd

in isolated cell walls and cells exposed to low temperatures. Observation of protoplasmic-dependent Cd accumulation in the cell wall challenges a primary assumption of previous research, that accumulation of Cd in the symplasm was entirely metabolism dependent, and accumulation of Cd in the apoplasm was entirely metabolism-independent. Dissection of the rate of Cd accumulation into a linear and a saturable component by Hart *et al.* (1998) is still a valid method, and the linear component could represent Cd accumulation in the apoplasm. However, the saturable portion could represent Cd accumulation in both the symplasm and the apoplasm. A direct measurement of Cd in the apoplasm and the symplasm is necessary to evaluate this finding at the tissue level.

My observations of Cd accumulation in the cell wall of *Chara corallina* also differed from current assessments with regard to the nature of association with cell wall components. Work in whole root tissues suggested that most apoplastic Cd was non-exchangeable, (Cataldo *et al.* 1983, Hart *et al.* 1998), while sequential desorption analysis suggested that all apoplasmic Cd was exchangeable (Rauser 1987, Blaudez *et al.* 2000). Exchange from the cell wall in both cases was suggested to be rapid, occurring over 30–60 minutes. Desorption of Cd from the cell wall of *Chara corallina* internodal cells was not as rapid as previously observed. Exchange always continued through the longest time points examined (3 or 12 hours). Results from these experiments were consistent with the suggestion that all cell wall Cd is exchangeable over time (Hart *et al.* 1998). However due to the length of time required, experiments testing this hypothesis were not conducted. I used non-linear regression analysis to model pool sizes and exchange constants from desorption curves. Results suggested two exchangeable pools (without a non-exchangeable component) provided the best fit. The most surprising aspect of this analysis was that pools of similar size were observed during desorption of intact and isolated cell walls. This indicated that both desorbable Cd pools (and the majority of desorbable Cd from intact cells) originated from the cell wall. Traditional interpretation of Cd desorption in *Chara corallina* would have assigned the fast desorbing component to the cell wall, and the slower desorbing component to the protoplasm.

A possible explanation for the differences in results can be found in the assumptions required to assign components of the desorption curve to specific subcellular locations. The sequential desorption technique was first utilized on another giant algae, *Nitellopsis obtusa* (MacRobbie and Dainty 1958). These authors examined movement of K^+ from internodal cells. They made direct observations of ions present in subcellular compartments and attributed certain pools within a sequential desorption curve to these components. It should be noted that the underlying assumption was that all three subcellular components act in series with one another. This technique was then used to study monovalent cation efflux in plant roots (Kochain and Lucas 1982). The same analysis was conducted on the desorption curve without the benefit of direct confirmation of cation location. The same technique, and interpretation, was later adapted to the study of divalent cation efflux from roots (Rauser 1987, Lasat *et al.* 1998, Blaudez *et al.* 2000), again without the direct confirmation of cation location. As monovalent and divalent cations have different accumulation patterns, it cannot be assumed that they would behave the same way during influx and efflux. This does not mean that desorption curves from previous experiments are not valid, however the interpretation of the results may need to be re-examined.

A new hypothesis can be proposed that places more emphasis on cation accumulation in the cell wall, including the presence of multiple binding sites with different cation affinities. The compartmental efflux model, which incorporates Cd efflux from the cell wall, cytoplasm, and vacuole, could be modified to suggest that the majority of desorbed Cd originated from different sites within the cell wall. Also, one or more of the exchanging Cd components could represent Cd originating from the apoplasm of cortex cells. This new model does not yet deal with Cd efflux from the protoplasm. Cadmium desorption was observed from the protoplasm of *Chara corallina*, but this desorption was masked by the variation present in the slower exchanging pool from the cell wall. A similar phenomenon could be occurring in the desorption profiles observed for roots or fungal mycelia. The ability to surgically isolate subcellular components from the *Chara corallina* system provides a direct measurement of Cd desorption from the protoplasm, a technique that was not available for studying Cd

accumulation in the symplasm of roots. Due to the lack of direct observation, desorption of symplasmic Cd would not be identified as a separate component of the desorption curve. Rather, the symplasmic component would exist within the variation observed from cell wall desorbing Cd. Direct measurements of Cd desorption from the apoplasm and symplasm are necessary for full evaluation of these suggestions.

The main difference between my analysis of Cd accumulation in the protoplasm of *Chara corallina* and previous studies was the degree to which the protoplasm is accessible to Cd. These studies (Hart *et al.* 1998, Cataldo *et al.* 1983, Lasat *et al.* 1998, Blaudez *et al.* 2000) suggested that approximately 50–70 % of accumulated Cd was localized to the symplasm of root tissue, while sequential desorption analysis suggests between 30 and 50% of divalent cations reaches the symplasm. In *Chara corallina*, accumulation in the protoplasm after 180 minutes accounted for 15% of total Cd at 1 nM exposure, and only 3% of total at 100 nM $CdCl_2$. Accumulation of Cd in internodal cells continued through 180 minutes at low concentrations (1 and 10 nM), but saturated after 90 minutes at 100 nM. It is possible that single internodal cells reached their maximal capacity to accumulate Cd around this concentration. Accumulation in the total protoplasm was equally divided between the avacuolate protoplasm and the vacuole at low concentrations over the 180-minute exposure period. The direct observation of Cd accumulation in the vacuole of *Chara corallina* internodal cells agrees with previous work suggesting the vacuole as a subcellular destination for divalent cations (Rauser 1987, Salt and Wagner 1993, Lasat *et al.* 1998, Blaudez *et al.* 2000). When the kinetics of Cd accumulation were examined, the Cd accumulation rate for the total protoplasm, the avacuolate protoplasm, and the vacuole each approached their calculated maximum (estimations of V_{max}: total protoplasm, $6.07 \pm 1.83 \times 10^{-13}$ moles mm^{-2} h^{-1} ; avacuolate protoplasm, $7.58 \pm 5.10 \times 10^{-13}$ moles mm^{-2} h^{-1} ; vacuole, $0.58 \pm 0.22 \times 10^{-13}$ moles mm^{-2} h^{-1}). However all K_m values had extremely high standard errors associated with them making interpretation of the kinetics unreliable.

Accumulation of Cd in the protoplasm appears to be dependent on cellular metabolism as exposure to Cd in conjunction with the metabolic inhibitors DNP or

CCCP reduced accumulation up to 75%. Cellular metabolism appears to play a general role in Cd accumulation as exposure at low temperatures reduced accumulation by 90%. However, due to the high standard error associated with the values, these differences were not statistically significant using Duncan's Multiple range test. These observations agree with the metabolism-dependence of symplasmic Cd accumulation suggested by previous research (Cataldo *et al.* 1983, Hart *et al.* 1998, Blaudez *et al.* 2000). The degree to which Cd can reach the symplasm still remains a question in the vascular plant systems used to date.

In a general sense, the basis for differences observed between this and previous studies could be explained by two possibilities. The first would be inter-specific differences between *Chara corallina* internodal cells and roots of vascular plants. To my knowledge, no research examining differences between the structural composition of the cell wall or plasma membrane for Characeae and vascular plants has been conducted. Nonetheless, we are still examining accumulation of a divalent cation in a single plant like cell that has a cell wall, a plasma membrane, and a tonoplast. The Characeae are the closest evolutionary relative to vascular plants as suggested by structural, biochemical, and molecular analysis (Chapman and Buchheim 1991, Graham *et al.*1991). In addition, results from studies using giant algal cells (*Nitellopsis*) provided a basis for further sequential desorption studies on plant roots, and laid the groundwork for development of the compartmental efflux interpretation. These similarities support use of this system as a model for a single vascular plant cell.

The second potential explanation for differences would be the fact that previous studies have examined Cd accumulation at an organ level and attempted to extrapolate the data to a single or subcellular level (Cataldo *et al.*1983, Hart *et al.* 1998). This approach may not be valid as the root as an organ contains numerous differentiated and undifferentiated cell types, which may have different patterns of Cd accumulation and efflux. For example, cells in the root cap region may have a different accumulation pattern than cells that have undergone differentiation. Also, cells located on the epidermal surface that encounter cations in the soil solution may have a different

accumulation pattern than cells located in the root cortex. Kinetic data accumulated from the tissue studies represent the average accumulation potential for all cells in the tissue, and not necessarily any single root cell. Of course, data on Cd accumulation from a single internodal cell of *Chara corallina* cannot be interpreted as representing any one of the root cell types described above. What these data do provide is a direct measurement of Cd accumulation at the single cell level and forms a platform from which to critically examine data collected through previous indirect approaches. My results suggest that re-evaluation of the current assumptions regarding Cd accumulation, the reliance on metabolism, and assignment of subcellular location are warranted.

A new approach (in the absence of techniques to directly observe plant cell Cd localization) to study accumulation of Cd and other divalent cations could involve the field of molecular biology. Numerous potential divalent cation transporters have been cloned (Clemens *et al.* 1998, Hirschi *et al.* 2000, Thomine *et al.* 2000) and these proteins appear to have varying affinities for different cations including Cd. The *Arabidopsis* gene *IRT1* is one such metal transporter (Roger *et al.* 2000). Single amino acid substitutions within this gene have altered the cation selectivity of the gene product when expressed in yeast (Rogers *et al.* 2000). A genetic approach (by amino acid level alterations or site directed mutagenesis) could be used to design divalent cation transporters that can have little or no affinity for Cd or other toxic metal ions while maintaining a high affinity for nutrient cations such as Zn or Mn. This might reduce uptake of Cd in the symplasm of plant tissues minimizing accumulation where Cd exposure to plants is highest. Another application of this approach might be to modify an existing metal ion transporter known to be present at the tonoplast (or any organelle membrane where Cd accumulation would not affect biological processes) to exclusively shuttle Cd into the vacuole (or organelle). This might sequester Cd and reduce its mobility throughout the remainder of the plant, further limiting Cd access to consumable organs. This approach would not only require expression of the modified gene, but the transcript would have to include an organelle specific targeting sequence as well. Until the physiology of Cd movement throughout crop plants, from root to shoot transport to loading in the consumable organs, is fully elucidated, the next best approach to

minimize human Cd exposure would be to minimize crop exposure, potentially through the methods discussed above.

The data presented in this thesis have allowed me to arrive at the following conclusions regarding Cd accumulation in subcellular components of *Chara corallina* internodal cells:

- the cell wall is the dominant point of localization for accumulated Cd,
- the accumulation pattern for Cd in the cell wall contains both a protoplasm-dependent and protoplasm-independent component,
- the protoplasm is accessible to Cd, and accumulation in the total protoplasm is equally divided between the avacuolate protoplasm and the vacuole,
- accumulation of Cd in the total protoplasm, the avacuolate protoplasm, and the vacuole appears metabolism dependent.

Examination of the nature of cell wall accumulation allowed me to come to the following conclusions:

- desorption of Cd from intact cells or post-exposure isolated cell walls occurs in a similar manner, suggesting that the majority of Cd desorbed from an intact cell originates in the cell wall
- all accumulated Cd is potentially exchangeable form the cell wall,
- a model suggesting two pools of exchangeable Cd provided the best interpretation for cell wall desorption results, suggesting multiple binding sites exist in the cell wall
- previous interpretation of divalent cation desorption profiles using the compartmental efflux interpretation may need to be re-examined.

These results have questioned some of the basic assumptions associated with previous research on the accumulation and desorption of divalent cations in vascular plants. While the systems used here is not entirely comparable, the results question interpretations of tissue data at the subcellular level. Re-examination of tissue data may be warranted.

4.2 References

Blaudez, D., Botton, B., Chalot, M. 2000. Cadmium uptake and subcellular compartmentation in the ectomycorrhizal fungus *Paxillus involutus*. Microbiology. 146: 1109-1117.

Cataldo, D.A., Garland, T.R., Wildung, R.E. 1983. Cadmium uptake kinetics in intact soybean plants. Plant Physiol. 73: 844-848.

Chapman, R.L., Buchheim, M.A.. 1991. Ribosomal RNA gene sequences: analysis and significance in the phylogeny and taxonomy of green algae. Crit. Rev. Plant Sci. 10: 343-368.

Clemens, S., Antosiewicz, D.M., Ward, J.M., Schachtman, D.P., Schroeder, J.I. 1998. The plant cDNA *LCT1* mediates the uptake of calcium and cadmium in yeast. Proc. Natl. Acad. Sci. 95: 12043-12048.

Graham, L.E., Delwiche, C.F., Mishler, B.D. 1991. Phylogenetic connections between the 'green algae' and the 'bryophytes'. Advances in Bryology. 4: 213-244.

Hart, J.J., Welch, R.M., Norvell, W.A., Sullivan, L.A., Kochain, L.V. 1998. Characterization of cadmium binding, uptake, and translocation in intact seedlings of bread and durum wheat cultivars. Plant Physiol. 116: 1413-1420.

Hirschi, K.D., Korenkov, V.D., Wilganowski, N.L., Wagner, G.J. 2000. Expression of *Arabidopsis CAX2* in tobacco. Altered metal accumulation and increased manganese tolerance. Plant. Physiol. 124: 125-133.

Kochain, L.V., Lucas, W.J. 1982. Potassium transport in corn roots. I. Resolution of kinetics into a saturable and linear component. Plant Physiol. 70: 1723-1731.

Lasat, M.M, Baker, A.J.M., Kochain, L.V. 1998. Altered Zn compartmentation in the root symplasm and stimulated Zn absorption into the leaf as mechanisms involved in Zn hyperaccumulation in *Thlaspi caerulescens*. Plant Physiol. 118: 875-883.

MacRobbie, E.A.C., Dainty, J. 1958. Ion transport in *Nitellopsis obtusa*. J. Gen. Physiol. 42: 335-353.

Rauser, W.E. 1987. Compartmental efflux analysis and removal of extracellular cadmium from roots. Plant Physiol. 85: 62-65.

Reid, R.J., Brookes, J.D., Tester, M.A., Smith, F.A. 1996. The mechanism of zinc uptake in plants. Characterisation of the low-affinity system. Planta. 198: 39-45.

Rogers, E.E., Eide, D.J., Guerinot, ML. 2000. Altered selectivity in an *Arabidopsis* metal transporter. Proc. Natl. Acad. Sci. 97: 12356-12360.

Salt, D.E., Wagner, G.J. 1993. Cadmium transport across tonoplast vesicles from oat roots. Evidence for a Cd^{2+}/H^{+} antiport activity. J. Biol. Chem. 268: 12297-12302.

Taylor, G.J., McDonald-Stephens, J.L., Hunter, D.B., Bertsch, P.M., Elmore, D., Rengel, Z., Reid, R.J. 2000. Direct measurement of aluminum uptake and distribution in single cells of *Chara corallina*. Plant Physiol. 123: 987-996.

Thomine, S., Wang, R., Ward, J.M., Crawford, N.M., Schroeder. J.I. 2000. Cadmium and iron transport by members of a plant metal transporter family in *Arabidopsis* with homology to *Nramp* genes. Proc. Natl. Acad. Sci. 97: 4991-4996.